MINISTRY OF EDUCATION AND SCIENCE OF UKRAINE

National University "Zaporizhzhya Polytechnic"

REVIEW
of the diploma project (work)

Variations in the geometry of the cross-sectional profile of the extruded filament using manufacturing method layer-by-layer welding up (FFF)

Student Larysa Hurina

Specialty 131 Applied mechanics

Project scope full
Number of drawings
Number of explanatory note sheets 74

a) short content of project (work) and decisions taken In this work literature study was provided, the influence of section location on the lengths of bond lines between and within layers was investigated,the effect of printing speed, extrusion multiplier and nozzle- bed distance on the cross-sectional geometry was revealed, labour protection and safety in the emergencies

b) conclusion about the conformity of the project to the task
The work is completely up to the task

c) completion characteristic of each section of the diploma project (work), level of compliance with the latest achievements of science and technology, advanced methods of work
The work corresponds to the latest achievements of science and technology at a sufficient level

d) negative features of project (work) implementation
no negative features were found

e) positive features The positive features can be considered: the influence of printing parameters on the formation of bonding between and within layers in FFF was detected, limit feed rate for certain parameters (layer height, nozzle diameter) was determined

e) evaluation of graphic design and explanatory note of the project (work) The presentation and explanatory note are in accordance with current standards

f) feedback on the project (work) in general In general, the master's work of the student of M-118m group of Hurina Larysa meets the requirements of the high school

g) other remarks It would be advisable to add porosity studies and strength tests

i) evaluation of the project (work) In general, the master's work of the student of the M-118m group of Hurina Larysa deserves a grade of "excellent"

The review was made by Associate Proffesor
of the engineering technology department Natalia Honchar

« 29 » 11 2019 y.

Форма № 31

МІНІСТЕРСТВО ОСВІТИ І НАУКИ УКРАЇНИ

Національний університет «Запорізька політехніка»

РЕЦЕНЗІЯ
на дипломний проект (роботу)

Варіації геометрії профілю поперечного перерізу екструдованої нитки при виготовленні методом пошарового наплавлення (FFF)

(вказати тему дипломного проекту (роботи))

Студент (ка) Гуріна Лариса Олександрівна

Спеціальність 131 Прикладна механіка

(код, найменування спеціальності)

Обсяг проекту повний

Кількість аркушів креслень —

Кількість сторінок пояснювальної записки 74

а) короткий зміст проекту (роботи) та прийнятих рішень У роботі проведено літературний огляд, досліджено впив розташування перерізу на довжину ліній склеювання між шарами та всередині шарів, досліджено вплив швидкості друку, екструзійного множника та відстані від платформи до сопла на геометрію поперечного перерізу, охорона праці та безпека у надзвичайних ситуаціях

б) висновок про відповідність проекту (роботи) завданню

Виконана робота повністю відповідає поставленому завданню

в) характеристика виконання кожного розділу дипломного проекту (роботи), рівень відповідності останнім досягненням науки та техніки і передовим методам роботи

Виконана робота на достатньому рівні відповідає останнім досягненням науки та техніки

г) негативні особливості виконання проекту (роботи)

При перевірці виконаної роботи негативних особливостей не виявлено

д) позитивні особливості Позитивною особливистю можна вважати: виявлено вплив параметрів друку на формування зв'язків між шарами за технологією пошарового наплавлення (FFF), визначено граничну швидкість друку для певних параметрів (висота шару, діаметр сопла) е) оцінка графічного оформлення та пояснювальної записки до проекту (роботи) Презентація та пояснювальна записка виконані у відповідності до діючих стандартів

є) відгук про проект (роботу) загалом В цілому магістерська робота студентки групи М-118м Гуріної Лариси Олександрівни відповідає вимогам вищої школи

ж) інші зауваження Було б доцільно додати дослідження пористості деталей та провести випробування на міцність

з) оцінка проекту (роботи) В цілому магістерська робота студентки групи М-118м Гуріної Лариси Олександрівни заслуговує оцінку «відмінно»

Рецензію склав доцент кафедри ТМБ Гончар Н.В.

(посада, місце роботи, прізвище, ім'я, по батькові) *(підпис)*

«29» 11 2019 р.

[13:05:03] Yah Найдено 2% совпадений по адресу: https://iopscience.iop.org/article/10.1088/1757-899X/479/1/012094/meta

[13:05:16] Go Найдено 1% совпадений по адресу: https://www.ncbi.nlm.nih.gov/pmc/articles/PMC6650798/

[13:05:17] Go Найдено 1% совпадений по адресу: https://link.springer.com/article/10.1007/s00170-019-03683-5

[13:05:19] Yah Найдено 1% совпадений по адресу: http://www.natureworksllc.com/~/media/Technical_Resources/Technical_Data_Sheets/TechnicalDataSheet_3D850_Monofilament_pdf.pdf?la=en

[13:05:24] Go Найдено 1% совпадений по адресу: https://link.springer.com/article/10.1007/s00170-018-03276-8

[13:05:37] Возникла ошибка при загрузке поисковой страницы №597 [3] (200029 миллисек.): Yandex (Время ожидания операции истекло)

[13:05:39] Bi Найдено 1% совпадений по адресу: https://link.springer.com/chapter/10.1007/978-3-319-91713-9_1

[13:06:12] Yah Найдено 1% совпадений по адресу: https://link.springer.com/article/10.1007/s00170-018-2586-5

[13:06:12] Yah Найдено 1% совпадений по адресу: https://www.sciencedirect.com/science/article/pii/S2214860417300465

[13:06:51] Возникла ошибка при загрузке поисковой страницы №592 [3] (200041 миллисек.): Yandex (Время ожидания операции истекло)

[13:07:50] Возникла ошибка при загрузке поисковой страницы №602 [3] (200045 миллисек.): Yandex (Время ожидания операции истекло)

[13:08:05] Возникла ошибка при загрузке поисковой страницы №607 [3] (200027 миллисек.): Yandex (Время ожидания операции истекло)

[13:09:12] Возникла ошибка при загрузке поисковой страницы №612 [3] (200032 миллисек.): Yandex (Время ожидания операции истекло)

[13:09:46] Возникла ошибка при загрузке поисковой страницы №622 [3] (200022 миллисек.): Yandex (Время ожидания операции истекло)

[13:09:50] Возникла ошибка при загрузке поисковой страницы №617 [3] (200022 миллисек.): Yandex (Время ожидания операции истекло)

[13:09:58] Возникла ошибка при загрузке поисковой страницы №627 [3] (200038 миллисек.): Yandex (Время ожидания операции истекло)

[13:10:56] Возникла ошибка при загрузке поисковой страницы №632 [3] (200017 миллисек.): Yandex (Время ожидания операции истекло)

[13:11:43] Возникла ошибка при загрузке поисковой страницы №642 [3] (200039 миллисек.): Yandex (Время ожидания операции истекло)

[13:11:59] Возникла ошибка при загрузке поисковой страницы №637 [3] (200039 миллисек.): Yandex (Время ожидания операции истекло)

[13:12:51] Возникла ошибка при загрузке поисковой страницы №647 [3] (200038 миллисек.): Yandex (Время ожидания операции истекло)

[13:14:06] Возникла ошибка при загрузке поисковой страницы №652 [3] (200047 миллисек.): Yandex (Время ожидания операции истекло)

[13:14:31] Возникла ошибка при загрузке поисковой страницы №657 [3] (200031 миллисек.): Yandex (Время ожидания операции истекло)

[13:15:58] Возникла ошибка при загрузке поисковой страницы №662 [3] (200015 миллисек.): Yandex (Время ожидания операции истекло)

[13:16:18] Возникла ошибка при загрузке поисковой страницы №667 [3] (200031 миллисек.): Yandex (Время ожидания операции истекло)

[13:16:51] Возникла ошибка при загрузке поисковой страницы №672 [3] (200042 миллисек.): Yandex (Время ожидания операции истекло)

[13:17:09] Возникла ошибка при загрузке поисковой страницы №677 [3] (200036 миллисек.): Yandex (Время ожидания операции истекло)

[13:17:10] Тип проверки: *Стандартная*

[13:17:10] **Уникальность текста 81%**©

MINISTRY OF EDUCATION AND SCIENCE OF UKRAINE
Zaporizhzhya Polytechnic National University

Machine construction
(full name of the institute, faculty)
Engineering technology
(full name of the department)

Explanatory note

to the diploma project (work)
master (second)
(degree of higher education)

on the topic Variations in the geometry of the cross-sectional profile of the extruded filament using manufacturing method layer-by-layer molding up (FDF)

Perform: student II term, group M-118m

Specialty 131 Applied mechanics
(code and name)

Educational program (specialization)
Engineering technology
Larysa Hurina
(surname and initials)
Supervisor Eduard Kondratiuk
(surname and initials)
Reviewer Nataliia Honchar
(surname and initials)

20 19

MINISTRY OF EDUCATION AND SCIENCE OF UKRAINE
Zaporizhzhya Polytechnic National University

Institute, faculty Machine construction
Department Engineering technology
Degree of higher education Master
Specialty 131 Applied mechanics
(code and name)
Educational program (specialization) Engineering technology
(name of educational program(specialization))

APPROVED
Head of department ET Dyadya S.
« 03 » 12 2019 year

TASK
OF THE STUDENT'S GRADUATE PROJECT (WORK)

Larysa Kuzina
(full name)

1. Theme of the project (work) Variations in the geometry of the cross-sectional profile of the extruded filament using manufacturing method layer-by-layer welding up (FFF)

supervisor of the project (work) Edward Kondratyuk, doct. of tech. sciences, prof.
(full name, scientific degree, academic title)

Approved by the order of higher education institution from «26» 11 2019 року № 416

2. Deadline for submission of the project (work) 22.11.2019
3. Background to the project (work) Investigation of features of parts manufacturing using fused filament fabrication (FFF)
4. Contents of the explanatory note (list of questions to be developed) 1) literature study; 2) Influence of section location on bond length; 3) Influence of printing speed; 4) Influence of extrusion multiplier; 5) Influence of nozzle-bed distance; 6) labour protection.
5. List of graphic material (with exact indication of mandatory drawings) presentation

6. Consultants of sections of the project (work)

Section	Surname, initials and position of the consultant	Signature, date	
		task issued	accepted the completed task
Research	Eduard Kondratiuk doctor of technical sciences, associate prof.		
Labour protection	Shmygko V. doctor of technical sciences, associate professor	4.10.19	29.11
Standards control	Lokominoo V. doctor of technical sciences associate professor		

7. Date of issue of the task « 01 » 10 2019 year.

CALENDAR PLAN

№	The stages` name of the graduation project (work)	Project implementation stages	Note
1	Literature study	08.10.2019	
2	Influence of section location on bond length	29.10.2019	
3	Influence of printing speed	05.11.2019	
4	Influence of extrusion multiplier	12.11.2019	
5.	Influence of nozzle-bed distance on cross-sectional profile	20.11.2019	
6	Labour protection and safety in emergencies	29.11.2019	

Student ____________ Hurina Larysa
(signature) (surname and initials)

Supervisor of the project (work) ____________ / Kondratiuk Edu
(signature) (surname and initials)

ABSTRACT

EN: 74 pages, 39 figures, 16 tables, 28 references.

The influence of the processing conditions on the cross-section profile of a strand printed by material extrusion additive manufacturing was investigated. The parts manufactured by this method generally suffer from a poor surface finish and a low index of strength, coming from the lack of control over the cross-sectional profile of the printed strands. Inter- and intra-layer bonds pose regions of weakness in structures produced via melt extrusion based polymer additive manufacturing. Bond strength was assessed both between layers and within layers as a function of print parameters.

The purpose of this master's thesis is to investigate the influence of printing conditions (distance between platform and nozzle, feed rate, print speed) on the geometry of the cross-section of the deposited filaments, the effect of temperature during deposition and the inter- and inter-layer connection between them.

The results of this work show the effect of printing parameters on the length of the inter-layer and inter-layer bond lines. The effect of the location of the cross-section regarding the effect of temperature was also observed. The contact length between the layers was measured with an optical microscope and with CT scan. The machine's maximum print speed was calculated for certain printing parameters.

FUSED FILAMENT FABRICATION, FUSED DEPOSITION MODELING, POLY (LACTIC ACID), BONDING FORMATION, INTRA-LAYER BOND LINE, INTER-LAYER BOND LINE, CROSS-SECTIONAL PROFILE

CONTENT

LIST OF ABBREVIATIONS

AM - Additive manufacturing

FFF -Fused filament fabrication

ABS -Acrylonitrile butadiene styrene

PLA - Poly (lactic acid)

FDM - Fused deposition modeling

SEM - Scanning electron microscope

NBD - Nozzle-bed distance

CT - Computed tomography

EM - Extrusion multiplier

ANOVA - Analysis of variance

INTRODUCTION

This master's thesis investigates the geometry of cross-sectional profile of extruded strand in fused filament fabrication (FFF), which is one kind of extrusion-based additive manufacturing technique, also known as 3D printing and fused deposition modeling (FDM).

For a particular polymeric material, the geometrical cross section is primarily determined by machine specifications and process parameters. Influential factors include (but not limited to) -nozzle-bed distance, printing speed, layer thickness, feed rate, etc. These factors affect the rheological properties and temperature of the extruded strand, which then will primarily determine the cross-sectional profile of printed parts.

This text reveals the pattern of cross-sectional profile variations with respect to the a few factors: 1. Nozzle-bed distance shift, 2. printing speed and 3. feed rate. The results will be important to further researches on temperature modeling and bond formation in FFF.

According to literatures, the deposition flow of the strands has an impact on the inter-layer bond formation in extrusion-based additive manufacturing, as well as the surface roughness of the fabricated part. The parts manufactured by this method generally suffer from a poor surface finish and a low dimensional accuracy, coming from the lack of control over the shape of the printed strands.

The fabrication time and the manufacturing resolution depend on the size and the shape of the extruded strands, which relate themselves to the processing conditions. The cross-section of the strand is also an important parameter for the bonding strength between the layers, as it determines the width of the bonding area [1]–[3]. Moreover, the strand profile affects the cooling rate of the part via heat conduction between the adjacent strands and layers [4]–[6]. Furthermore, knowledge about the strand shape allows better control of the part porosity[1] and its mechanical properties [7].

A literature review on the statistical relations between the extrusion conditions and the properties of the final parts was made in [8]. It was found that the mechanical properties are strongly correlated to the layer thickness, the build orientation, and the infill density of the parts. The surface roughness is significantly influenced by the layer thickness and the build orientation.

Serdeczny et al. [9] investigated experimentally and numerically the influence of the processing conditions on the cross-section of a strand printed by material extrusion additive manufacturing. Depending on the processing conditions, the cross-section of the strand can vary from being almost circular to an elongated rectangular shape with rounded edges. For all the measurements, decreasing the gap height deforms the strand and changes its shape from an oval (for a large gap height), to a flat cuboid with rounded corners (for a small gap height). Decreasing the velocity ratio leads to an increase in the cross-sectional area of the strand as more material is deposited per unit distance of the strand (the extrusion volumetric flux is constant).The deposition of multiple strand layers and their cross-section have not been researched.

The goal of this master thesis is to investigate the influence of printing conditions (nozzle-bed distance, feed rate, printing speed) on the geometry of cross-section of the deposited strands, temperature during deposition and intra- and inter-layer bonding between them.

1 LITERATURE STUDY

1.1 Introduction

In material extrusion Additive Manufacturing (AM), also known as fused filament fabrication or fused deposition modeling, a semi-liquid material is extruded through a nozzle and selectively deposited in the form of a strand, to create the layers of a sliced three-dimensional object.

The parts manufactured by material extrusion AM used to be primarily employed for prototyping and rapid tooling; however, their areas of application as finished components have broadened every year as the process more frequently meets the stringent requirements to deliver end-use products [10], [11]. The most common material extrusion AM machines use thermoplastics, where the feedstock is a solid filament fed into a liquefier that melts the material before the extrusion [12]. The extruded strands bond to the previously deposited material by the mean of a temperature-driven diffusion process [2].

The material extrusion AM process is often more economical than other AM techniques [12] and easier to use as the popular build materials are non-toxic [13]. AM technologies are especially attractive in applications with low volumes of production and complex geometries.

However, the components produced by material extrusion AM have anisotropic mechanical properties that are affected by the build orientation of the part [14] and the tool path calculated by the slicing software. Another inherent feature of the layered-based manufacturing methods is that the finished parts have rough surfaces, which are more difficult to post-process in the case of thermoplastics than for metals [12]. Therefore, the processing conditions must be well controlled for an optimal rendering of the surfaces[15], [16].

The FFF process is controlled by many parameters, the parameters play an important role in ensuring surface quality and mechanical properties of the final part. Therefore, the selection of appropriate parameters is the key to successful printing. Many researches were focused on the optimization of the process parameters and explored the relationship between process parameters and the final product quality. Anitha et al. [17] studied the effects of process parameters including road width, thickness, and printing speed on the surface quality of ABS part. They found that the layer thickness is the main influencing factor of the surface quality, which become worse with layer thickness increases. Christiyan et al. [18] investigated the effect of layer thickness and printing speed on the tensile and flexural strength. It was found that low layer thickness and low printing speed can improve the tensile and flexural strength due to sufficient adhesion between layers. Sood et al. [19] studied the effect of part orientation, layer thickness, raster angle, part raster width and raster-to-raster gap on the quality of printing parts.

The above studies indicate that the layer thickness is important on the surface finish and mechanical strength of FFF parts. However, these studies are all based on a default thickness of the nethermost first layer, i.e. the nozzle-bed distance (NBD) (Fig.1.1). The NBD value has been suggested to be effective for the good adhesion of the manufactured part with the building platform. Ravi et al. [21] provided the only report on NBD on strut width by printing single-layer scaffolds aiming at control the printing accuracy. However, the influence of NBD on the bonding formation were not reported.

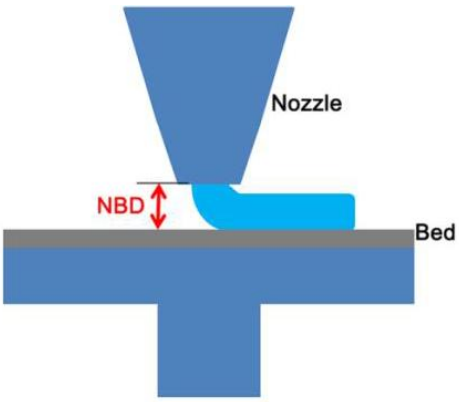

Figure 1.1- Illustration of the nozzle-bed distance parameter

Among many process parameters, the strand-to-strand distance is a crucial for the porosity [1] and the mechanical strength of fabricated parts [7]. The layer thickness and the extrusion flow rate also have an influence on the tensile strength, as they affect the shape of strands and thereby the bonding areas [1],[22]. The influence of the layer thickness and extrusion flow rate on the strand shape and the force exerted on the substrate by the extruded material was reported in [23].

1.2 Describing the mesostructure of FFF material

Rodriguez, James and Renaud [1] have identified that the mesostructure of a FFF material is the main contributor to its mechanical properties. The mesostructure is the material's structure at the medium level scale, in which the geometry of the filaments, the voids and the bonds is described. The model used by Rodriguez, James and Renaud [1] to characterize the mesostructure assumes the filament's initial cross sectional shape to be an ellipse.The main dimensions of these ellipses are the horizontal (semi-major) axis and the vertical (semi-minor) axis.

The most curious variables for this ellipse model are the horizontal and vertical gap, which are the differences between width and height of the "ellipse" and the true filament width and layer thickness respectively. A positive gap, which is only physically possible in the horizontal direction, means that the ellipses do not touch as depicted in Fig. 1.4 by Li et al. [7], resulting in zero transverse mechanical strength and stiffness. With a negative gap the ellipses touch more intimately as shown in Fig. 1.2 by Li et al. [7], where a is the ellipse' semi-major (horizontal) axis, b- the ellipse' semi-minor (vertical) axis, Δ -the horizontal negative gap. A similar graph can be constructed for the vertical overlap, depicted in Fig.1.3, with δ as the vertical gap.

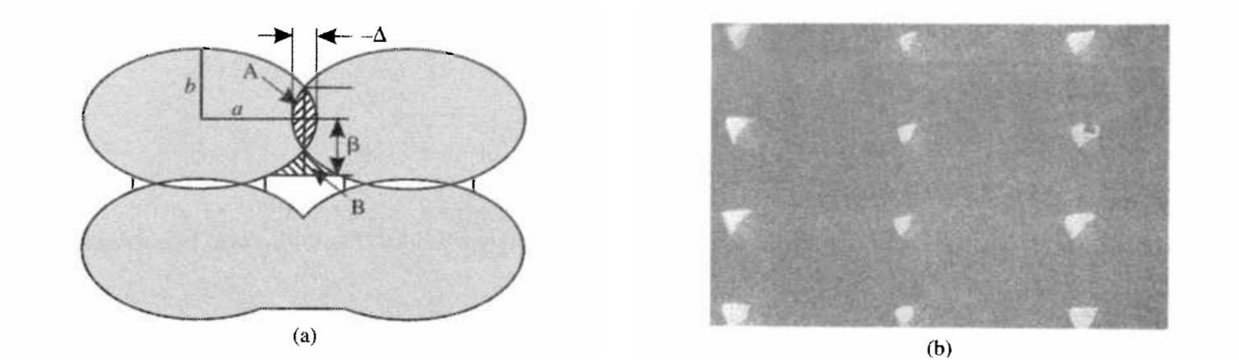

Figure 1.2 - (a) Model of mesostructure as proposed by Li et al. [7]; (b) cross sectional SEM photo of mesostructure by Li et al. [7]

The ellipse model makes sense when the horizontal gap is positive or zero, as shown in Fig. 1.3. The negative gap is the only setting which leads to meaningful mechanical properties in transverse direction. However, the SEM images in Fig. 1.3 are more akin quadrangles with rounded corners. In the mesostructural model proposed by Li et al. [7] the overlapping material between the two ellipses flows into the adjacent voids, resulting in lower void density and filling the sharp void corners.

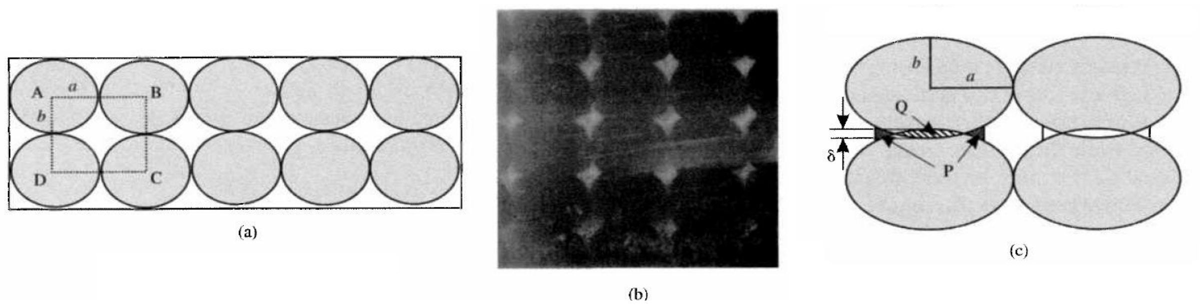

Figure 1.3 - (a) Control volume of one void as shown by Li et al. [7]; (b) cross sectional SEM photo of mesostructure by Li et al. [7]; (c) model of mesostructure as proposed by Li et al. [7]

Note that with zero or positive overlap, the bond length is also theoretically zero, as shown by Li et al. [7] in Fig. 1.4. From a mechanical perspective this case would result in zero stiffness and strength in the transverse direction. This means that the bonds form a very important factor in the mechanical properties of FFF materials. Describing the bond lengths using the print settings, the part dimensions and the part weight will give a very useful tool predicting the mesostructure for mechanical analysis.

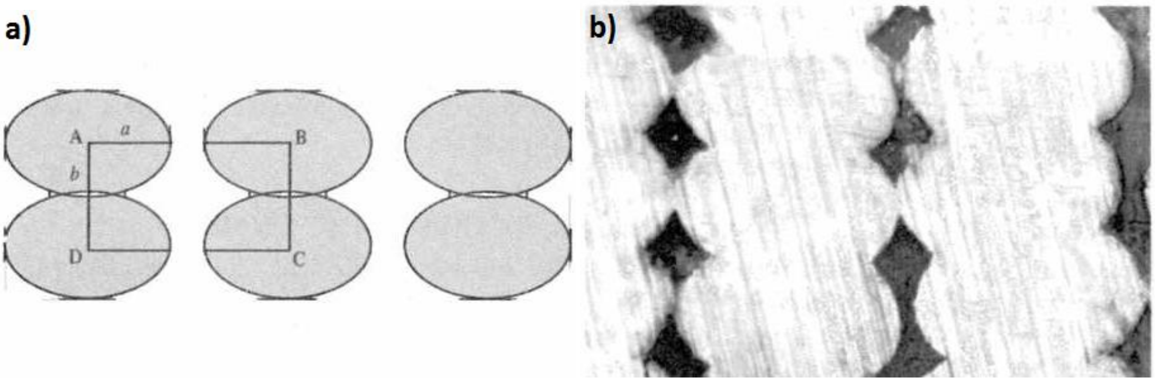

Figure 1.4 - (a) Model of mesostructural as proposed by Li et al. [7]; (b) cross sectional photo of mesostructure with positive vertical gap by Li et al. [7]

It was determined by Rodriguez, James and Renaud [1] that a myriad of variables have an effect on the mesostructure. The manufacturing parameters which were found to have an impact on the mesostructure are: the extrusion temperature, the envelope temperature, the fiber-to-fiber gap, extrusion flow rate, increment nozzle height, nozzle speed and fiber path width direction. Rodriguez, James and Renaud [1] found that the material to be anisotropic due to the presence of long continuous voids in the lengthwise filament direction, where in the lengthwise filament direction the material is stiffer as compared to the transverse direction.

Rodriguez, James and Renaud [1] found that the filament gap was very determining towards the bond length, which in part is very important for the mechanical characteristics in transverse tension and shear. However, attempts to bring the void density to zero led to extruder jamming and material defects and is therefore not desirable.

1.3 Conclusion

Despite the large success of the FFF process, there are still many challenges that need to be addressed to ensure its competitiveness. In general, FFF parts have a smaller tensile strength than components fabricated with conventional manufacturing techniques like for instance injection molding. The reduced strength is attributed to the weak inter- and intra-layer bonding and the presence of voids in the final product [14]. A mesostructure with large voids results in a small contact area between the strands and poor bonding. The porosity of fabricated parts is inherent to extrusion-based additive manufacturing and needs to be addressed at the stage of material deposition by choosing appropriately the process conditions [1]. Understanding the development of voids is essential for improving the mechanical strength of the parts, and to enable the production of components with locally controlled properties [7].

Most studies showed that the mechanical properties of the parts were negatively influenced by the insufficient bond strength achieved between filaments, the weak interlayer strength in the building direction often being the weakest and most critical link in the FDM parts.

It was felt that there is a scarcity of data on the mechanism of bond formation between adjacent filaments making up FDM parts. Therefore, considerable research effort is still needed to fully understand the effects of material and processing parameters on the bonding formation.

It is the goal of this work to research cross-sectional geometry profile of deposited strand, influence of printing parameters on cross-sectional geometry and bonding between adjacent strands. Since no such clear link has been made before.

2 MATERIALS AND METHODS

2.1 Materials and equipment

All 3D printed samples were manufactured by Prusa i3 MK3. The Slic3r PE software was used to slice the CAD model and prepared the G-Code for 3D printing. Technical data are: print size millimeters (xyz) 250 x 210 x 200 mm; accuracy 10 x 10 x 5 microns; layer height 50 microns; feeder system direct; extruder type single; nozzle size 0.4 mm; max extruder temperature 300 °C; max heated bed temperature 120 °C; max print speed 200 mm/s; bed leveling fully automatic. A double wall (2 tracks) sample geometry, 18×0.8×12 mm^3 was used for this work (Fig. 2.1). FFF setting are as summarized in Table 2.1.

Table 2.1 - Parameter setting for sample printing

Parameters	Values
Model dimension $L \times W \times H$	18×0.8×12 mm^3
Layer thickness Δh	0.3mm
Printing speed v	20 mm/s
Nozzle temperature T_n (nominal)	215 °C
Platform temperature T_p (nominal)	60°C
Air temperature T_a	21°C
Fan speed	On- max speed
Nozzle diameter (E3D V6 nozzle type)	0.4 mm
PLA filament diameter (PRUSA supplier)	1.75 mm

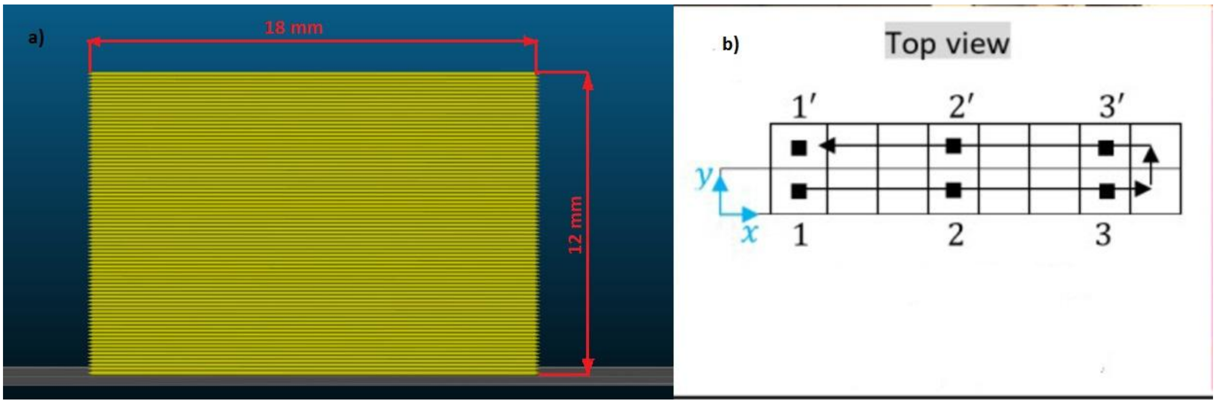

Figure 2.1- (a) the geometry of sample; (b) deposition sequence

The poly(lactic acid) (PLA) filament was used in this research. The filament was purchased from Prusa. (Prusa filament). Prusa used natureworks 4043D raw PLA for filament production. Material properties are as given in Table 2.2.

Table 2.2 - Properties of PLA [24]

Properties	PLA
Tensile strength	60 MPa
Elongation	6%
Flexural modulus	3.8 GPa
Density	1.23 -1.25 g/cm^3
Melting point	145-160°C
Glass transition temperature	55-60°C
Biodegradable	Yes, under the correct conditions

2.2 Resin embedment and microscope observation

To study the geometry of the samples Resin Embedment Experiment was done.

Materials was used for this experiment:

- Own samples;
- Sample Holder (Multiclips, etc);
- Resin and resin hardener;
- Resin containers;
- Vaseline, syringes and stirring stick;
- Curing Vacuum tool;

Procedure is describing below:

- Find the correct orientation of the samples and their samples holder;
- Insert the sample in the sample container;
- Put a bit of Vaseline with a stick to the edges of the container and on the bottom;
- Fill the container with resin and hardener → 15:2=resin: hardener;
- Insert the sample in the vacuum machine: curing vacuum for 10h. Wait until the end of the process.

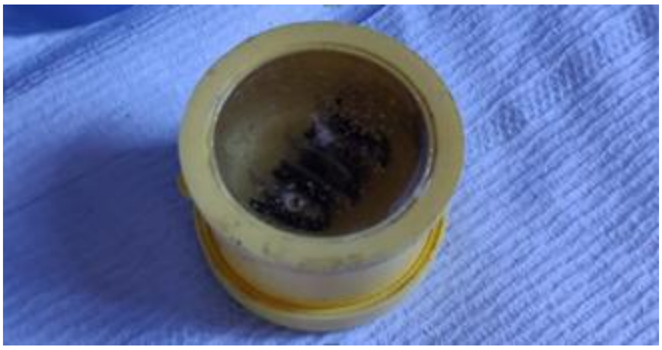

Figure 2.2 - The samples prepared for polishing

After the end of resin embedment (Fig. 2.2), grinding and polishing were applied for further research under microscope. Knuth-rotor 6X was used for grinding. Grinding paper ranging from grit 80 to grit 4000 can be used. To achieve smoother surface diamond polishing on AP 1 8X was provided using a diamond suspension 6 + H_2O μm and in the end of process 1 μm + H_2O.

The optical microscope, often referred to as the light microscope, is a type of microscope that commonly uses visible light and a system of lenses to magnify images of small objects. The image from an optical microscope can be captured by normal, photosensitive cameras to generate a micrograph. Purely digital microscopes are now available which use a CCD camera to examine a sample, showing the resulting image directly on a computer screen without the need for eyepieces.

The Keyence VH-ZST (Fig.2.3) was used for observing cross-section. This microscope integrates the next-generation adaptive multi-lighting, advanced auto-focusing and high-definition imaging. Featuring lens which can reach a range of magnification from 20x to 2000x.

Figure 2.3 - The microscope Keyence VH-ZST

Lower magnification (20 – 200x) objective was applied. This works well for flat specimens such as concrete thin sections; components embedded in epoxy, polished, and prepared for failure analysis and others.

2.3 Computed tomography scanning

A CT scan, also known as computed tomography scan, and formerly known as a computerized axial tomography scan or CAT scan, makes use of computer-processed combinations of many X-ray measurements taken from different angles to produce cross-sectional (tomographic) images of specific areas of a scanned object, allowing the user to see inside the object without cutting.

The geometry of the samples was investigated using Nikon XT H225ST(Fig.2.4). Detailed capture and measurement of internal component and assembly features is often vital for quality control, failure analysis and material research. XT H 225ST offers a powerful micro-focus X-ray source, a large inspection volume, and high X-ray and CT imaging resolution. XT H 225ST suits a wide range of applications, including inspection of small castings, plastic parts as well as material research.

Features: powerful 225kV micro-focus source with optional rotating target; real-time X-ray visualization; fast CT reconstruction; 5-axis fully programmable part manipulator; customizable macros automate measurement workflow; small footprint and castors & roller for easy handling. The settings of Nikon XT H225ST are as follows: focal spot size 8 μm, resolution 11-15μm. The GOM Inspect software was used to analyze of the data from Nikon XT H225ST. The lengths of the distance from bottom, intra- and inter-layer bond lines were measured and statistically compared.

Figure 2.4 - CT system Nikon XT H225ST: 1) stop panel; 2) manipulator; 3) sample-loading door; 4) “X-ray ON” Lamp; 5) X-ray source; 6) service access panel; 7) manual joystick controls; 8) LCD monitors

2.4 Experiments on cross -sections profile at different locations

To investigate cross-sections profile at different location the sample was printed with parameters specified in Table 2.1.

The fabricated sample was cut along the relevant *y-z* planes in 5 different places (Fig.2.6); the resin embedment and polishing of the cross sections were conducted and then inspected under a microscope (Fig.2.5). CT scanning of the sample also was made.

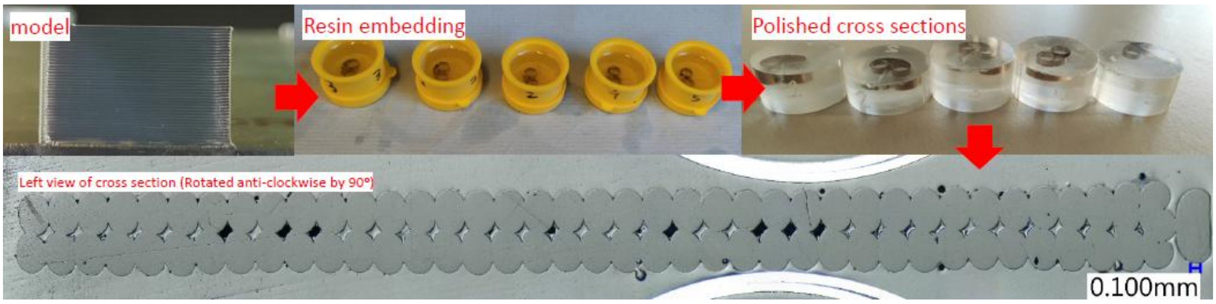

Figure 2.5 - Procedure of preparing the sample

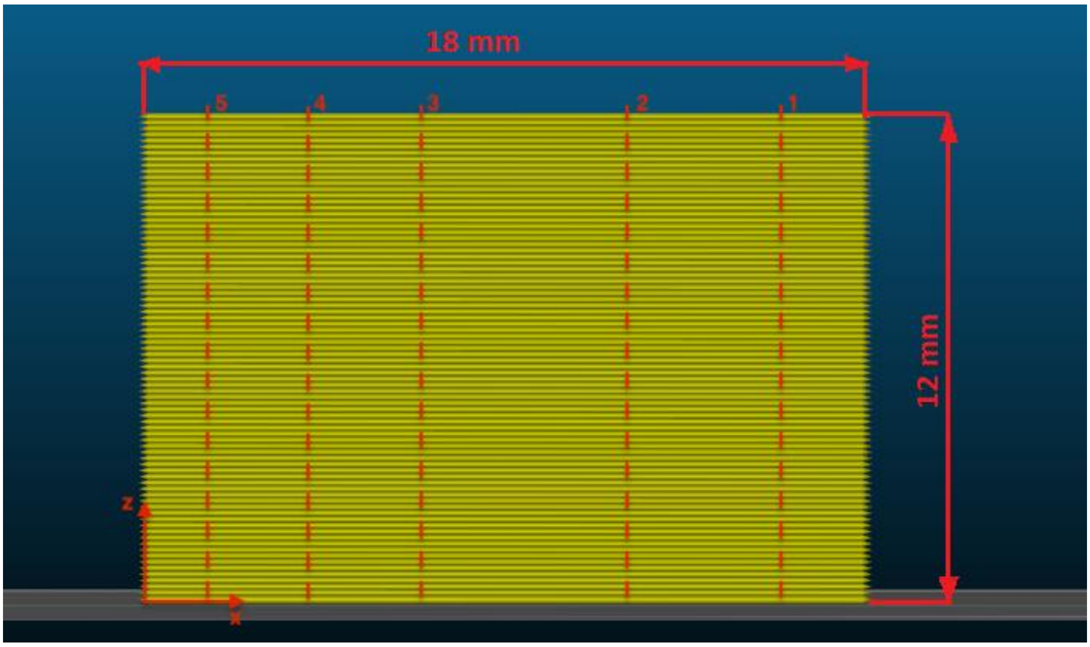

Figure 2.6 - The depiction of cross-sections

2.5 Experiments on cross-section profile at different printing speeds

To study the influence of printing speed on the bonding formation, one more experiment was conducted. There were two samples printed with different speed: 10mm/s and 20 mm/s (other printing parameters in section 2.1). The inspection under optical microscope and CT scanning were applied to research the cross-section of the specimens.

2.6 Experiments on cross- sections profile at different multipliers

2.6.1 Flow rate measurement

15(x3) samples with different value of extrusion multiplier (EM) were prepared with green PLA for this research. All printing parameters and geometry of samples are as given in section 2.1. It was started with EM equaled 0.3 and it was failure, 0.4 is minimum value of EM. It reached value of 16. The geometry of the samples was distorted beginning with EM equaled 3. The mass of all samples was measured with help the weighing scale Analytical Balance with 0.0001 g resolution.

2.6.2 The cross- section profiles at different multiplier

This part of experiment was devoted to effect of extrusion multiplier on the shape of strand in FFF.

Extrusion Multiplier allows to control how much filament comes out of the nozzle and make small adjustments to the extrusion flow rate. Increasing of multiplier from 1.0 to 1.05 leads to extruding 5% more filament.

To investigate the shape of strands 5 samples with different value of multiplier (0.7; 0.9; 1; 1.1; 1.5) were chosen and printed with transparent PLA. The resin embedment and polishing were applied and then observation under optical microscope.

2.7 Experiments on cross-sections profile at different NBD

Illustration of the NBD parameter was shown in Fig. 1.1. In this work the effect of NBD shift on cross-section profile of deposited strands was determined. Three values of NBD shift were chosen. As shown in Fig.1.1 the NBD shift equals 0, i.e. without any shift. Because the first layer will not well cohere with the building platform at large NBD, the shrinkage can lead to a failure of printing. The maximum NBD shift without warping deformation was 0.80 mm in this study. The minimum NBD shift was taken -0.3, because decreasing this value is inefficiently (it is impossible to descend below heating bed). Other printing parameters are as given in Table 2.1. For consistence, all samples were printed with transparent PLA in the middle of the building platform with one sample at a time.

3 EXPERIMENTAL RESULTS AND DISCUSSION

3.1 Influence of cross section location on bond length

The lengths of the intra-layer bond lines and inter-layer bond lines (Fig.3.1) were measured and statistically compared. The inter-layer bond lines in this work can be either early or late, depending on the sequence of deposition. Figure 3.1 shows the layers in the order of deposition. Table 3.1 and Fig.3.2 lists the lengths of intra-layer bond lines obtained. It shows that the lengths of intra-layer bond lines were different in each cross-section; the differences are statistically significant.

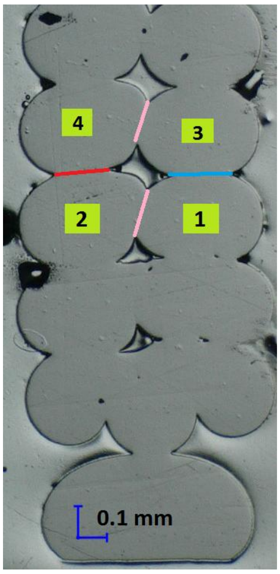

Figure 3.1 - The picture of cross-section with marked: pink lines -intra-layer bond lines; blue line-inter-layer bond lines early; red line-inter-layer bond lines late

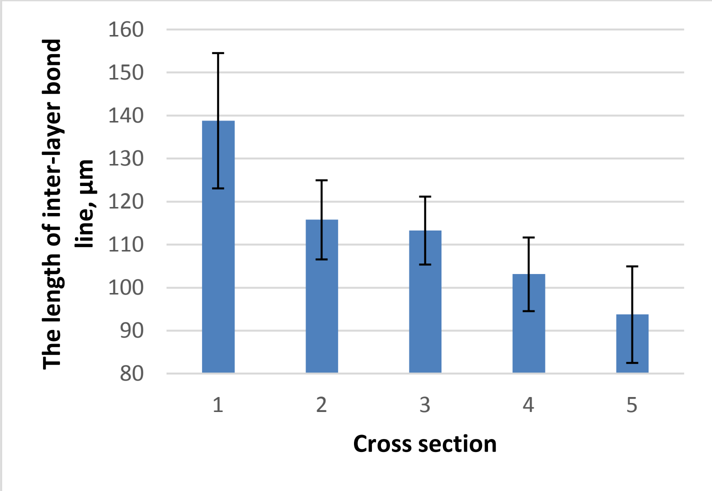

Figure 3.2 - Intra-layer bond length in 5 cross-sections (Fig.2.6)

Table 3.1- The lengths of intra-layer bond lines

Cross-section	1	2	3	4	5
X coordinate (mm)	16.72	11.91	6.16	4.80	1.29
Average length, µm	138,80	115,79	113,29	103,13	93,76
Standard deviation, µm	15,72	9,19	7,89	8,55	11,22

3.1.1 Analysis of variance

Analysis of variance was applied to determine the differences are significant.

Analysis of variance (ANOVA) is a collection of statistical models and their associated estimation procedures (such as the “variation” among and between groups) used to analyze the differences among group means in a sample. In the ANOVA setting, the observed variance in a particular variable is partitioned into components attributable to different sources of variation. In its simplest form, ANOVA provides a statistical test of whether the means of several groups are equal. ANOVA is useful for comparing (testing) three or more group means for statistical significance.

A test result (calculated from the null hypothesis and the sample) is called statistically significant if it is deemed unlikely to have occurred by chance, assuming the truth of the null hypothesis. A statistically significant result, when a probability (p-value) is less than a pre-specified threshold (significance level), justifies the rejection of the null hypothesis, but only if a priori probability of the null hypothesis is not high.

In the typical application of ANOVA, the null hypothesis is that all groups are random samples from the same population. Rejecting the null hypothesis is taken to mean that the differences in observed effects between groups are unlikely to be due to random chance.

A single factor or one-way ANOVA was used to test the null hypothesis that the means of several samples are all equal. Microsoft Excel was used.

H_0: $\mu_1 = \mu_2 = \mu_3 = \mu_4 = \mu_5$.

H_1: at least one of the means is different.

Table 3.2- Results of ANOVA for five cross-sections

Groups	Score	sum	The average	Dispersion
Cross-section 1	38	5275	138,8	247,0
Cross-section 2	38	4400	115,8	84,5
Cross-section 3	38	4305	113,3	62,3
Cross-section 4	38	3919	103,1	73,2
Cross-section 5	38	3563	93,8	125,8

Table 3.3- Results of Variance analysis

Source of variation	SS	df	MS	F	F critical
among groups	43386,6	4,0	10846,6	91,5	2,4
within groups	21933,1	185,0	118,5		

Conclusion: if F > F crit, the null hypothesis(H_0)is rejected. This is the case, 91.49 > 2.42. Therefore, the null hypothesis(H_0) is rejected. The means of the five samples are not all equal. At least one of the means is different. However, the ANOVA does not tell us where the difference lies. The t-Test is required to test each pair of means.

3.1.2 F-test

An F-test is any statistical test in which the test statistic has an F-distribution under the null hypothesis. It is most often used when comparing statistical models that have been fitted to a data set, in order to identify the model that best fits the population from which the data were sampled. Exact "F-tests" mainly arise when the models have been fitted to the data using least squares. The name was coined by George W. Snedecor, in honour of Sir Ronald A. Fisher. Fisher initially developed the statistic as the variance ratio in the 1920s.

Before using t-Test it is useful to determine which one is suitable (t-Test: Two-sample Assuming Unequal Variances or Assuming Equal Variances). F-Test was used to determine if the variances of the two samples are equal. Microsoft Excel was used.

H_0: $\sigma_{x-1}^2 = \sigma_x^2$.

H_1: $\sigma_{x-1}^2 \neq \sigma_x^2$.

Table 3.4- Results of F-test

Variances	1-2	2-3	3-4	4-5
F	2,92	1,36	1,17	1,71
F critical one-tail	1,73			

Conclusion: if F > F Critical one-tail, the null hypothesis(H_0)is rejected. This is the case only for variances 1-2, 2.923 > 1.729. Therefore, the null hypothesis(H_0) is rejected. The variances of the two cross-sections are unequal. In all other cases, the null hypothesis is not rejected, that means the variances are equal.

3.1.3 T-test

The t-test is any statistical hypothesis test in which the test statistic follows a Student's t-distribution under the null hypothesis.

A t-test is most commonly applied when the test statistic would follow a normal distribution if the value of a scaling term in the test statistic were known. When the scaling term is unknown and is replaced by an estimate based on the data, the test statistics (under certain conditions) follow a Student's t distribution.

The t-Test was used to test the null hypothesis that the means of two cross-sections were equal. Microsoft Excel was used.

H_0: $\mu_{x-1} - \mu_x = 0$.

H_1: $\mu_{x-1} - \mu_x \neq 0$.

Table 3.5- Results of t-test

Variances	1-2	2-3	3-4	4-5
t-statistics	7,8	1,3	5,4	4,1
t Critical two-tail	2,0			

Conclusion: The two-tail test (inequality) was made. lf t Stat < -t Critical two-tail or t Stat > t Critical two-tail, the null hypothesis(H_0) is rejected. This is the case for Variances 1-2, 3-4, 4-5. Therefore, the null hypothesis(H_0) is rejected. This is not the case for Variances 2-3. Therefore, reject the null hypothesis(H_0) is not rejected.

There is conclusion that all five cross-sections have different length of intra-layer bond lines except cross-section 2 and 3, the observed difference between these cross-sections means (115.79 – 113.3) is not convincing enough to say that the average length of intra-layer bond lines differ significantly. These differences are reasonable. It shows that the plane characterized by the shortest intra-layer time presents the longest bond lines. Contrary to the left side of the sample, the first re-heating takes place quickly after deposition at the right side, due to the short intra-layer time; the material remains "hot" for a relatively long period. This type of temperature profile should be representative of a long bond line between adjacent tracks.[25]

The lengths of inter-layer bond lines (early) and inter-layer bond lines (late) were investigated at the cross-section 1. Table 3.6 lists the results obtained.

Table 3.6 - The lengths of intra- and inter-layer bond lines

	Inter-layer bond line (early)	Intra-layer bond line	Inter-layer bond line (late)
Average length, µm	175,0	135,2	204,2
Standard deviation, µm	25,8	27,1	21

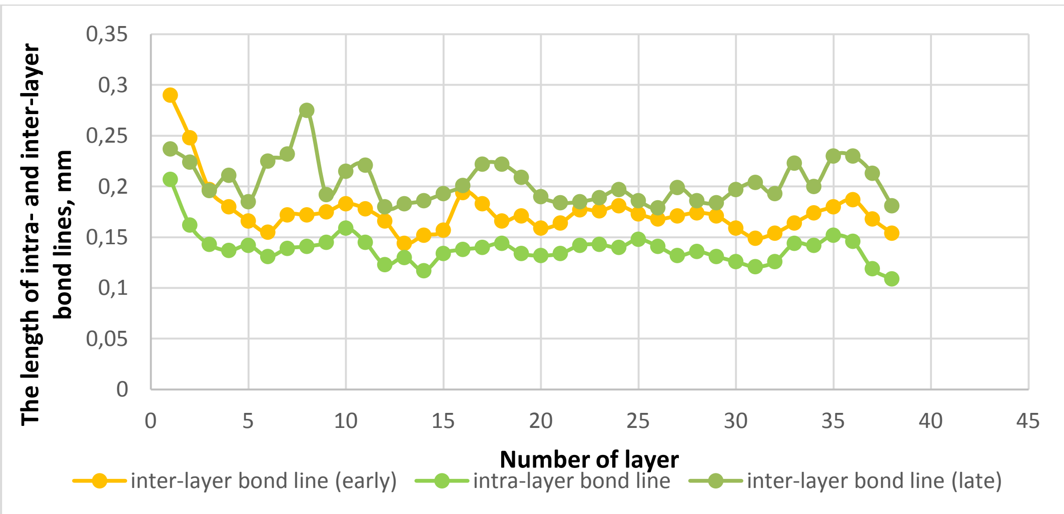

Figure 3.3 - The diagram of the lengths of inter- and intra-layer bond lines

F-test and t-test were used for verification of equal or unequal variances

Conclusion: if F > F Critical one-tail, the null hypothesis(H_0) is rejected. This is not the case, it was obtained 1.510<1.729. So, the null hypothesis(H_0) is not rejected. The variances of the two(early and late) depositions are equal.

The two-tail test (inequality) was made. lf t Stat < -t Critical two-tail or t Stat > t Critical two-tail, the null hypothesis(H_0) is rejected. This is the case, it was obtained -5.389 <-1.992. Therefore, the null hypothesis(H_0) is rejected.

It can be seen that lengths of inter-layer bond lines are different in early and late depositions. In general after 3 layers the lengths of inter-layer bond lines(late) are longer than inter-layer bond lines (early)(Fig.3.3).

It is relative to heat transfer between adjacent filaments. The late deposition layer interacts with two neighbors while the early one-with one neighbor. But the heat transfer between environment and filament must be taken into account. The temperature of environment is near 20°C, it is colder than T of deposited strand. As early deposited strand has more interaction with environment, it cools down faster. This would lead to conclusion that adhesion between early deposition layers is not so good because of fast cooling down in comparison with late ones.

3.1.4 Computed tomography scanning results

Computed tomography scanning was made for this sample. The sample was cut in 5 different locations [2.7 mm (5); 6.3 mm (4); 9.7 mm (3); 12.3 mm (2); 16.3 mm (1)] and observation of intra-layer bond and inter-layer bond lines was made.

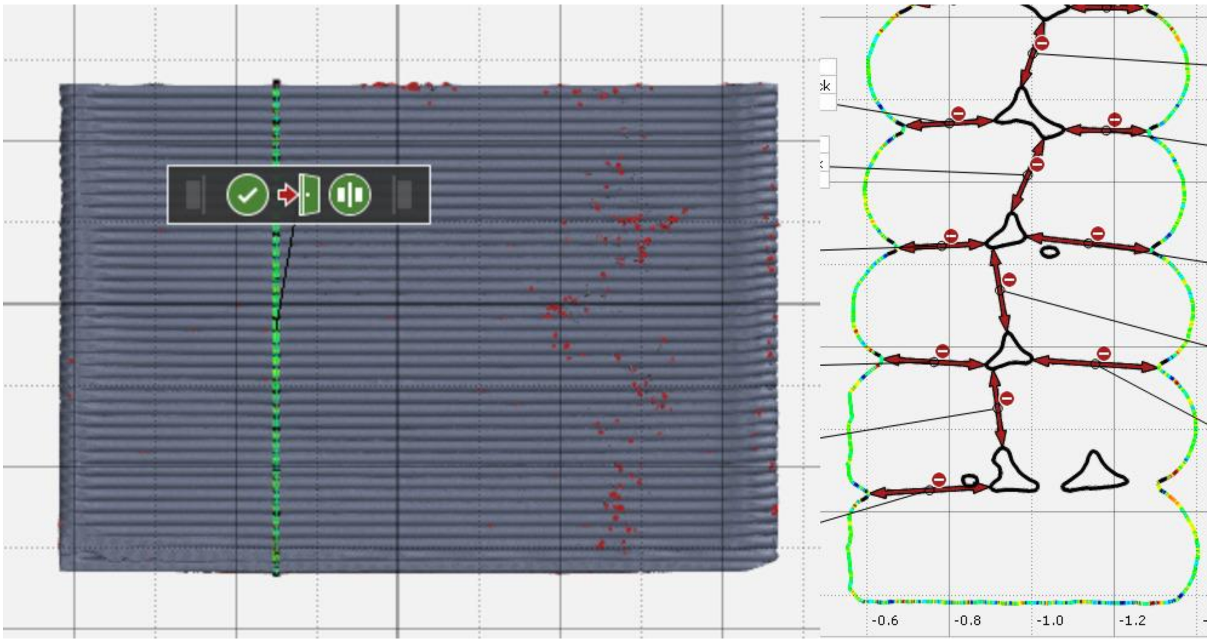

Figure 3.4 - The cross-section 4 in GOM software

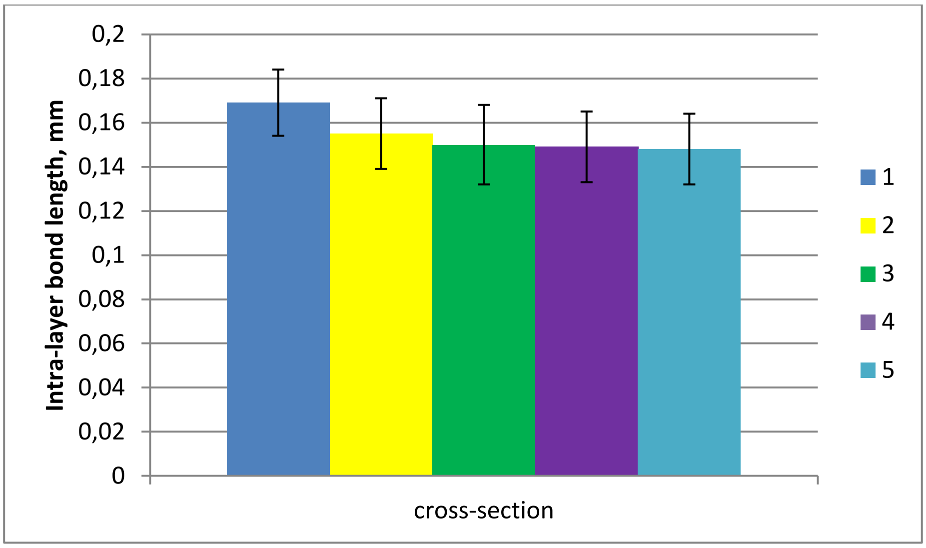

Figure 3.5 -Intra-layer bond length of five cross-sections by CT scanning

Table 3.7 -The results of measurement in CT scanning

cross-section		intra-layer bond	inter-layer bond later	intra-layer bond earlier
1 (16.3 mm)	Average length, µm	169	200	200
	Standard deviation, µm	15	20	22
2 (12.3 mm)	Average length, µm	155	187	183
	Standard deviation, µm	16	27	33
3 (9.7 mm)	Average length, µm	150	180	174
	Standard deviation, µm	18	25	36
4 (6.3 mm)	Average length, µm	149	184	169
	Standard deviation, µm	16	30	27
5 (2.7 mm)	Average length, µm	148	182	153
	Standard deviation, µm	16	32	27

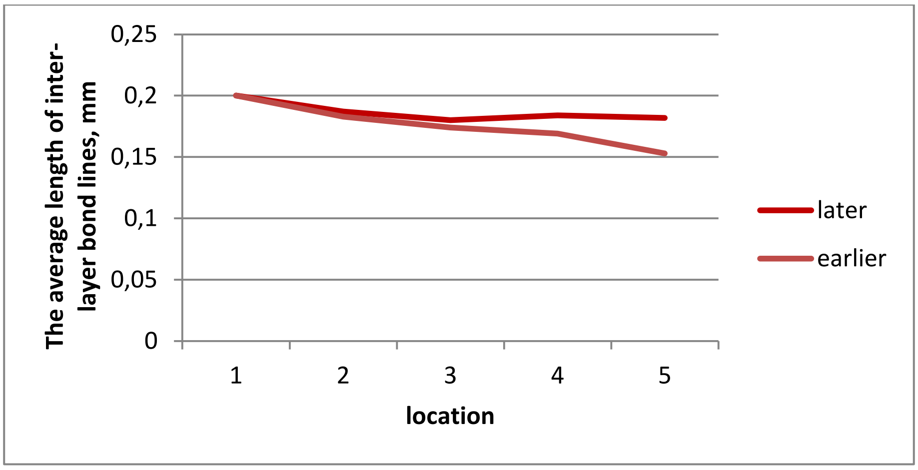

Figure 3.6 - The average length of intra-layer earlier and later bond lines of five cross-sections

By comparing of data from microscope and CT scanning, it was determined that data from CT scan was higher than data from microscope.

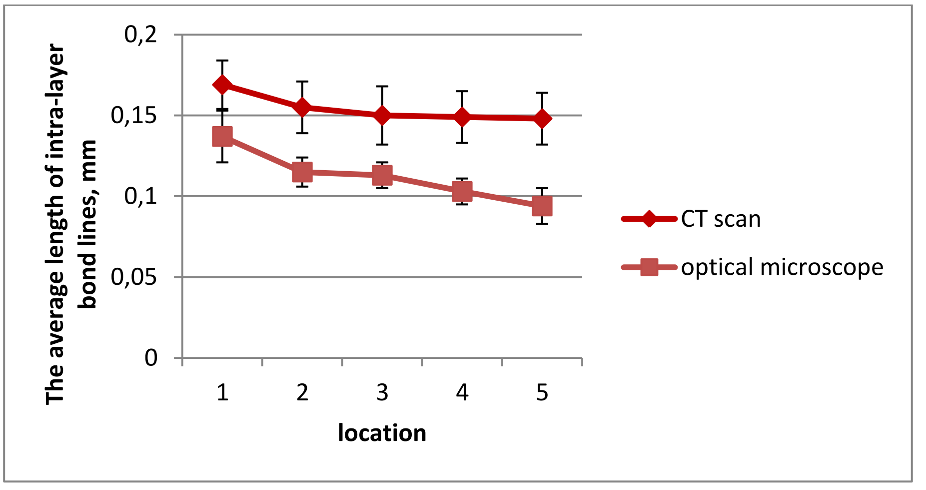

Figure 3.7 - The graph of comparing data from optical microscope and CT scan

The inaccuracy in CT scan can be considered. The focal spot size is an important factor for obtaining readable images in radiography. The focal spot size 8 μm was applied in this experiment. The results in CT depends on how the boundary is determined. Current setting for boundary detection gives a bigger boundary (Fig.3.8).

Figure 3.8-The influence of focal spot size on the CT scan accuracy

3.2 Influence of printing speed

Linear printing speed can have the least predictable effect on layer cohesion out of all factors considered in this paper. On one hand, increasing linear velocity also leads to an increase in the volumetric printing speed (flow rate, the volume of plastic extruded through the nozzle per unit of time). Thus, with increasing printing speed, the resistance to extrusion increases, which, obviously, will adversely affect the part mass. But printing speeds set in this work were not high and had not significant distinction (10 and 20 mm/s), though affect on the part mass was not considered.

On the other hand, the higher the printing speed, the sooner the next layer is printed and the less the sublayer cools before the new layer is deposited. In this sense, increasing the printing speed can have a similar effect to decreasing cooling intensity and, thus, it will contribute to an increase in the cohesive strength between the layers.

The measurement of intra-layer bond lines and inter-layer bond lines were done. The results of measurement of samples (10 mm/s) were represented in section 3.1.

Table 3.8 lists result of measurement of intra-layer bond lines of sample (20 mm/s).

Table 3.8 - The results of measurement of intra-layer bond lines of sample (20 mm/s) under microscope

Cross-section	1	2	3	4	5
Average length, μm	133,60	118,81	111,03	109,21	108,05
Standard deviation, μm	14,91	6,55	11,49	8,74	7,04

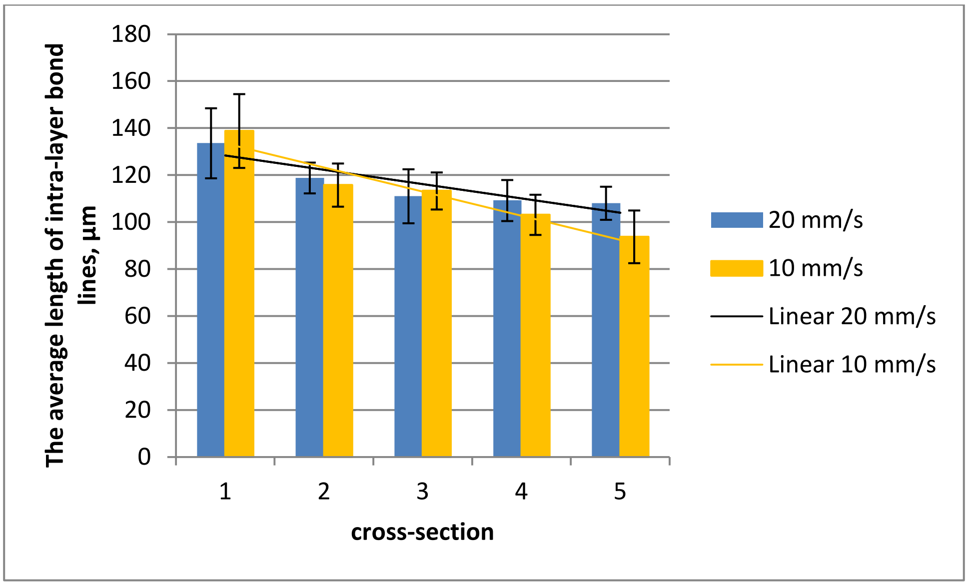

Figure 3.9- The graph of comparing the average length of intra-layer bond lines of samples with different printing speed

The data of average lengths of inter-layer bond lines in Fig.3.10 are obtained from analysis of cross-section 5.

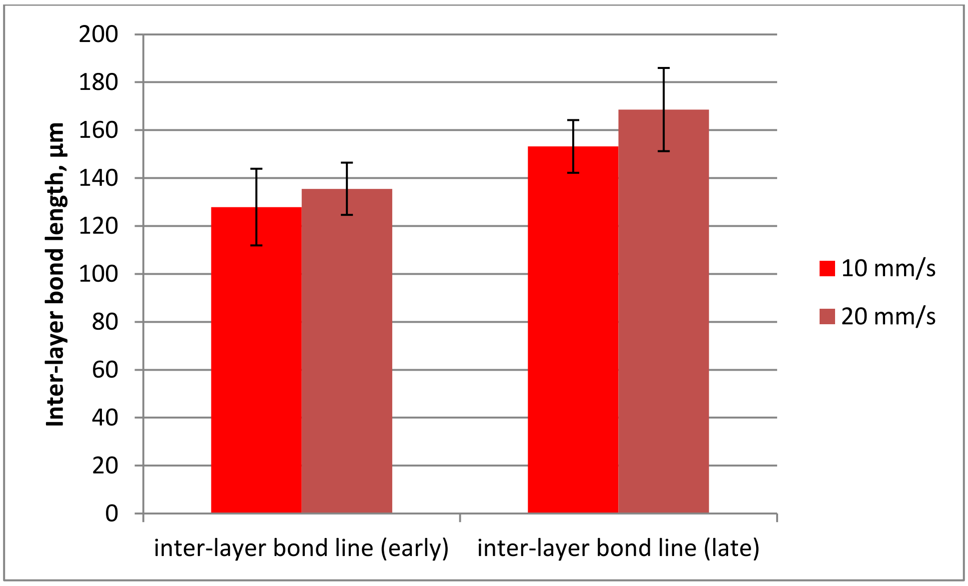

Figure 3.10- The graph of comparing lengths of inter-layer bond lines of samples with different printing speed

Print speed was expected to affect the thermal history of bond lines. Depositing molten polymer was expected to reheat both adjacent and underlying bond lines through radiation and conduction. Reheating would temporarily accelerate polymer diffusion and entanglement. In this way, bond formation would intermittently progress in response to reheating from continued road deposition during a print. As shown in Fig.3.9 the average length of intra-layer bond lines at all cross-sections for 20 mm/s speed are generally higher than for 10 mm/s. The reason of it is cooling down of earlier deposited strand by that time when later deposited strand will reach that point, that is why the adhesion between strands in cross-section 5 for 10 mm/s is weaker (Fig.3.11).

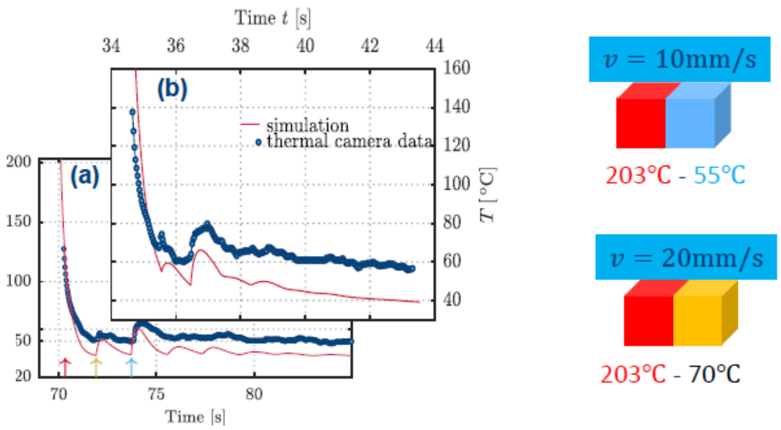

Figure 3.11- Temperature in different printing speeds

3.2.1 CT scanning results

CT scanning also was made to investigate the cross-sections of the samples. It was observed in the cross-section 5 of the sample (Fig.3.12).

The cross-sectionals profiles were represented in Fig.3.13. The average length of intra-layer bond lines of sample printed at speed 20 mm/s exceeds the average length of intra-layer bond lines at 10 mm/s (Fig.3.14).The reason of this was explained above.

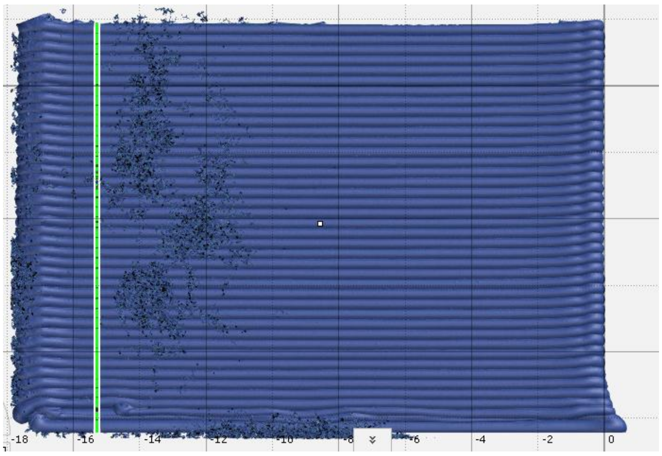

Figure 3.12 - The cutting plane (cross-section 5)

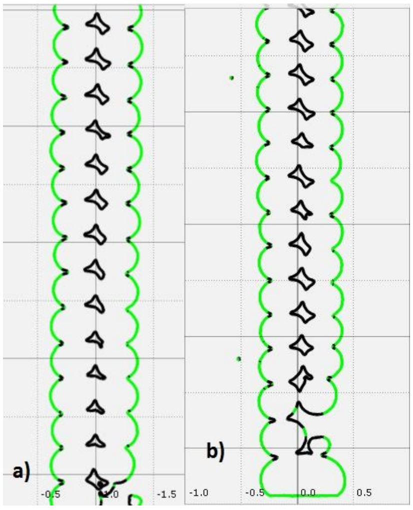

Figure 3.13 - The cross-sections of the samples: a) 10 mm/s; b) 20 mm/s

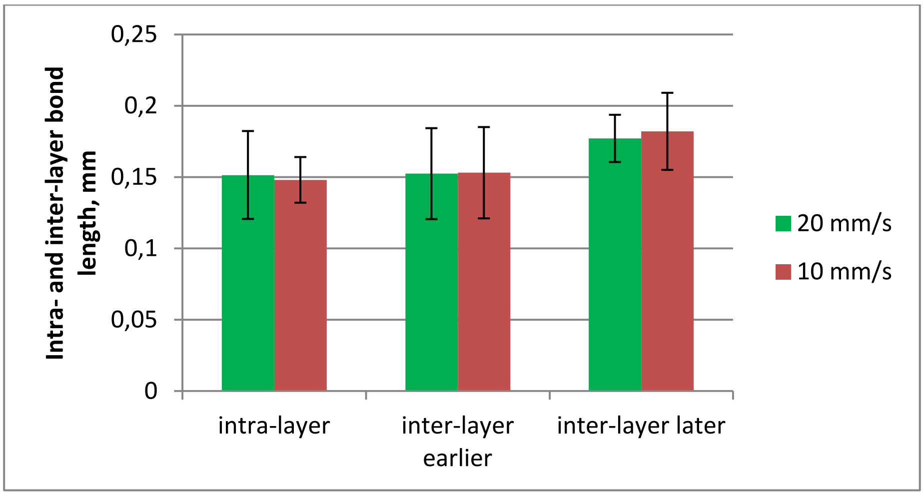

Figure 3.14- Length of intra- and inter-layer bond lines of samples printed with different speed

3.3 Influence of multiplier (flow rate)

3.3.1 Definition of limit printing speed

15(x3) samples with different multiplier were made in green PLA and were weighed. Printing time was 121 seconds. It was expected that with increasing extrusion multiplier the weight of samples would increase also. It would be explained by that fact that higher EM, more material is fed per second. The results of weighing are represented in Table 3.9. Three specimens of each multiplier were weighed and the average number was obtained. The mass flow rate was calculated according to the formula:

Mass flow rate = mass/ printing time, [g/s]

When EM equals 1, it is optimal case. For this case it was obtained mass flow rate = 6 g/h. Therefore the machine prints 6 grams of material per one hour. It was accepted as standard. The expected mass flow rate of each EM was calculated by multiplying value of extrusion multiplier by 6.

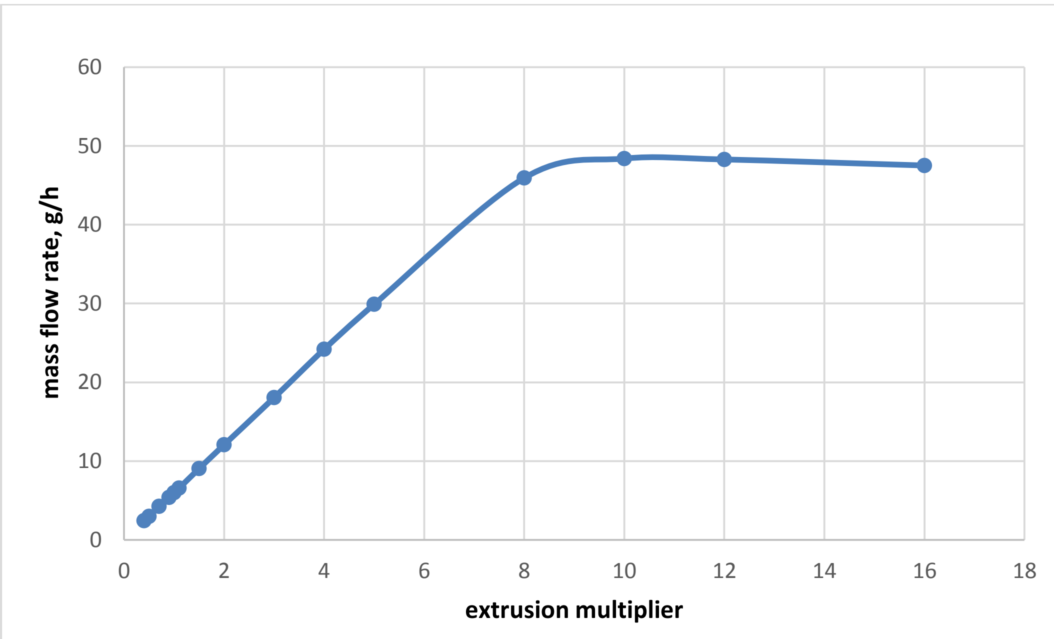

Figure 3.15 -Actual mass flow rate with different EM

Table 3.9- Results of samples weighing

EM	0.4	0.5	0.7	0.9	1	1.1	1.5
The average mass, g	0.08	0.10	0.14	0.18	0.20	0.22	0.30
Standard deviation, g	0.0009	0.0004	0.0005	0.0001	0.0004	0.0003	0.0007
Mass flow rate, g/h	2.44	2.99	4.26	5.39	6,00	6.58	9.06
Expected mass flow rate, g/h	2.4	3.0	4.2	5.4	6.0	6.6	9.0

Continuation of Table3.9

EM	2	3	4	5	8	10	12	16
The average mass, g	0.40	0.60	0.80	1.00	1.54	1.63	1.62	1.60
Standard deviation, g	0.003	0.0008	0.0027	0.006	0.03	0.003	0.008	0.005
Mass flow rate, g/h	12.08	18.06	24.20	29.90	45.90	48.39	48.28	47.51
Expected mass flow rate, g/h	12.0	18.0	24.0	30.0	48.0	60.0	72.0	96.0

The curve of actual mass flow rate behave not that way was expected. Starting with extrusion multiplier equals 8, actual mass flow rate is significantly lower than expected mass flow rate. From this point the limit value of printing speed for this machine can be calculated using actual mass flow rate of value of extrusion multiplier 8 because of from this point the curve does not change significantly.

$$Limit\ print\ speed = \frac{mass\ flow\ rate}{3.6 \cdot density \cdot nozzle\ diameter \cdot layer\ height}, [mm/s]$$

$$Limit\ print\ speed = \frac{45.9}{3.6 \cdot 1.24 \cdot 0.4 \cdot 0.3} = 85.68, [mm/s]$$

The conclusion is that the machine can not print higher than 85.68 mm/s for layer height 0.3 mm, if feed rate will be higher, it might lead to jamming or another defect. That is why the mass and therefore mass flow rate does not change. But there is 200 mm/s max speed of Pusa i3 MK3, it is possible to print at this speed with max layer height 0.12 mm.

Also without changing the temperature of the heating block, increasing the flow rate can lead to a decrease in the temperature of the plastic at the nozzle outlet - the plastic can be fed through the hot end so quickly that it will be able to melt, but will not be able to heat up to the temperature of the heating block due to lower exposure time.

3.3.2 Distinction between transparent and green PLA

The five samples were printed with different EM with transparent PLA for further research under microscope. They were also weighed (Table 3.10).

Table 3.10- The results of weighing transparent samples

EM	0,7	0,9	1	1,1	2
The average mass, g	0,140	0,178	0,199	0,220	0,397

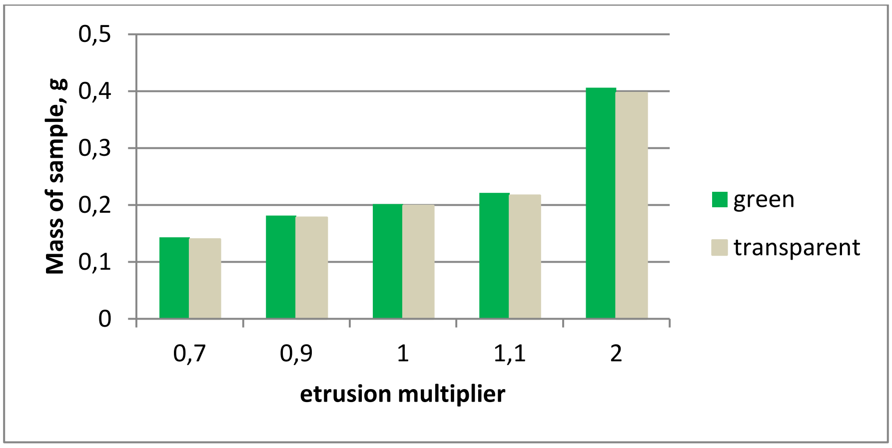

Figure 3.16- The graph of comparing mass’ of samples printed with green and transparent PLA

PLA has a semicrystalline structure and is a glossy, stiff and colorless polymer. To color the PLA, ink additives (tints or pigments) are added to its formulation, which can might change the polymer’s rheological properties. Often, the polymer’s color is not considered to be a factor that can influence the printing parameters. Nevertheless, according to some authors, the effects of PLA color on the 3D printed properties must affect the final characteristics of the polymer [26]. The results presented in [26] clearly show that percent crystallinity of 3D printed parts is color dependent. Natural PLA (no dye added) contains the lowest percent of crystalline regions with 0.93%. In contrast the white material was shown to include the greatest percentage of crystalline regions with 5.05%. All results in [27] demonstrate that transparent PLA should be preferred in color mixing processes by considering the performance of the ink since it changes the printability and rheological properties of the ink to a lesser degree. Referring to [27] adding color fragments usually decrease material viscosity. Lower viscosity corresponds to higher flow rate, consequently parts made with green PLA has greater value of mass.

3.3.3 Influence of extrusion multiplier on wall cross-section

The resin embedment for five transparent samples was done. The specimens were grinded by half, polishing and cross-sections were investigated under microscope. The outer thickness of each sample was determined.

For EM 1 the thickness of the sample should be 0,8 mm because it was determined by the geometry of the wall. It was obtained 0.84 mm thickness of the wall (Fig.3.17).

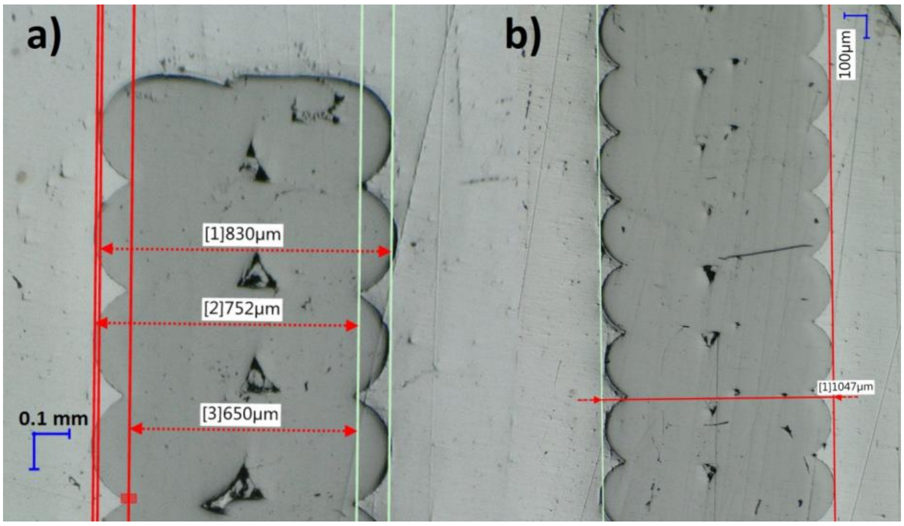

Figure 3.17 - The depiction of: a) outer, inner and medium thickness of sample with extrusion multiplier 1; b) outer thickness of sample with EM 1.5

Table 3.11- Thickness of the wall at different EM

EM	1,5	1,1	1	0,9	0,7
Thickness, μm	1054,7	920,7	838,3	777,3	643,0
Standard deviation, μm	14,1	9,0	7,2	15,5	24,0

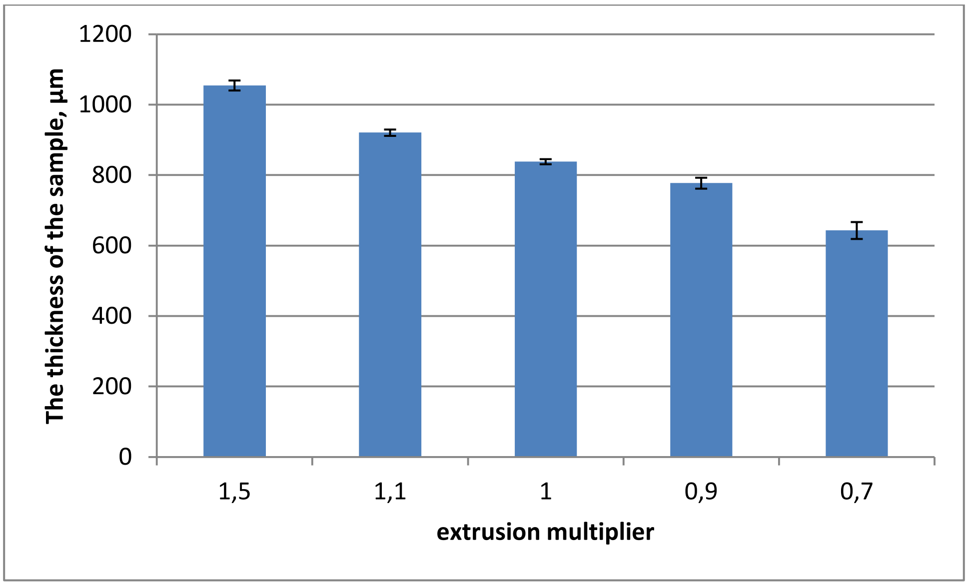

Figure 3.18- Thickness of the wall at different EM

As shown on Fig.3.18 the thickness grows with increasing extrusion multiplier. The layer height is 0,3 mm for all values of EM, but amount of material feeding through the nozzle is greater, consequently the material is distributed in width. And therefore it was obtained wider wall at bigger value of EM. The opposite case at smaller EM, less width of samples was obtained.

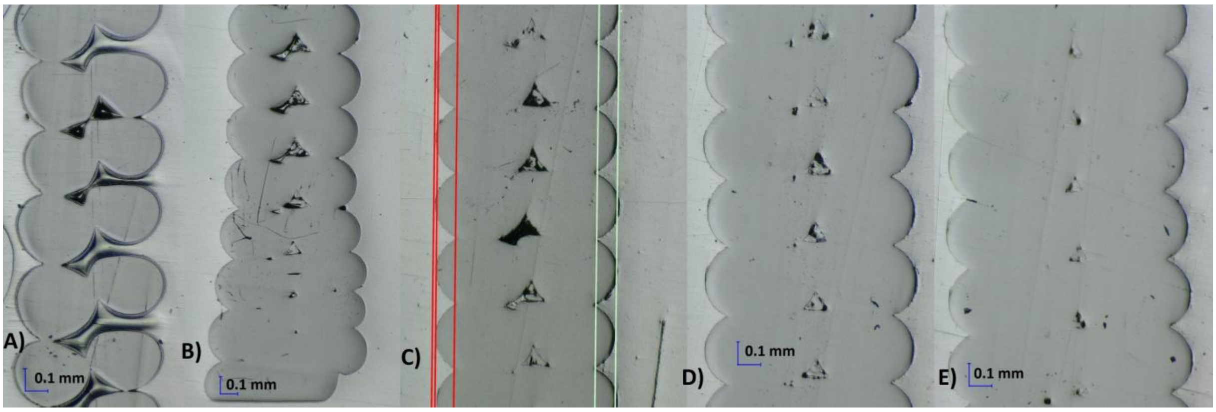

Figure 3.19-The cross-section profile of: A) extrusion multiplier 0.7; B) EM 0.9; C) EM 1; D) EM 1.1; E) EM 1.5

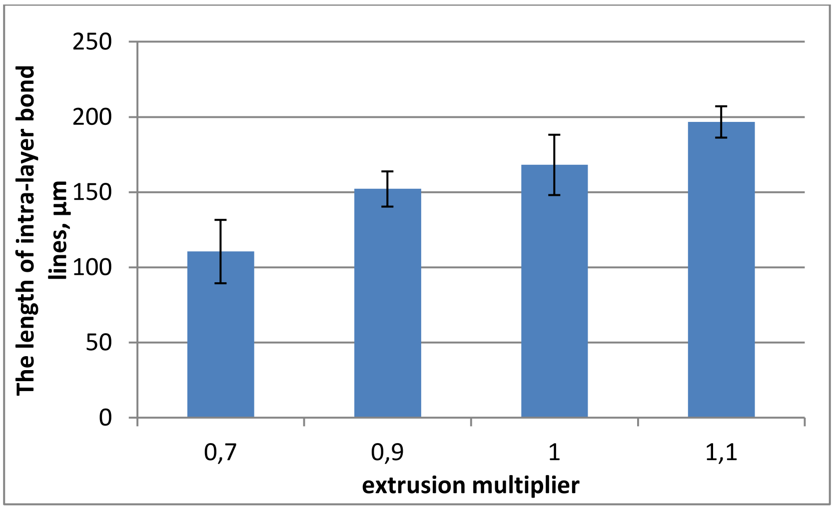

Figure 3.20- The length of intra-layer bond lines at different EM

The cross-section profiles are represented in Fig. 3.19.The lengths of intra-layer bond lines were measured (Fig.3.20). The lengths of intra-layer bond lines at EM 1.5 were not obtained, because it was difficult to determine their location. As shown in Fig.3.19 the voids at EM 1.5 almost disappear. This sample has dense structure and less percent of porosity, but it overstates the width of the wall. Some features can be seen at EM 0.7. The later deposited layers do not touch each other in many positions.

The extrusion multiplier parameter influences the amount of material extruded in the unit of length travelled by extruder with given speed, it's default value is 1. Extrusion multiplier influences all types of layers and fillings at the same time, changing the surface of cross-section of extruded filament thread because of affecting extrusion pressure. If set above 1, it allows creating more dense prints, but too high values can sometimes cause material overflow the defined shape of printed element, resulting in lowering dimensional accuracy but stronger prints. In opposite case, with extrusion multiplier <1, the resulting print is created with less than optimal amount of filament, resulting in worse bonding. Lesser bonding between strands of specimens stems from smaller diameter of extruded material filament and consequently, smaller surface of contact between neighbouring strands.

Four layers of each sample were not analyzed. The load of claps which were necessary for holding of samples during resin embedment experiment deforms the samples shape (Fig.3.21).

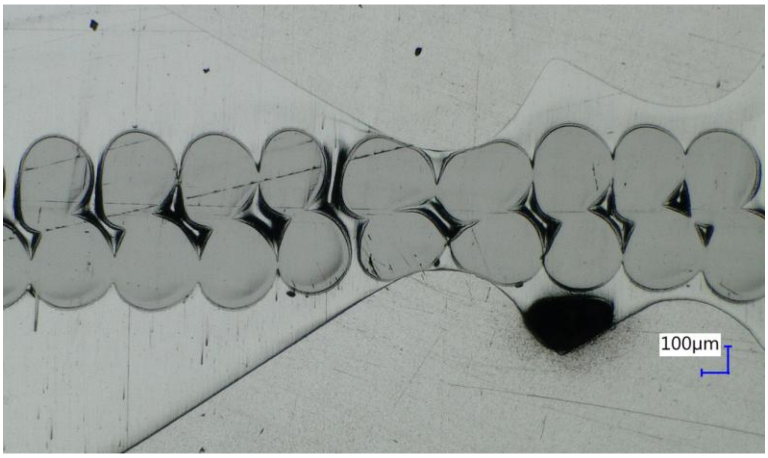

Fig.3.21- The depiction of deformation because of clamping

3.4 Influence of nozzle-bed distance shift on cross section profile

The data received from CT machine were processed in GOM Inspector software. The scanned specimens were cut in the middle and the cross-sections were investigated.

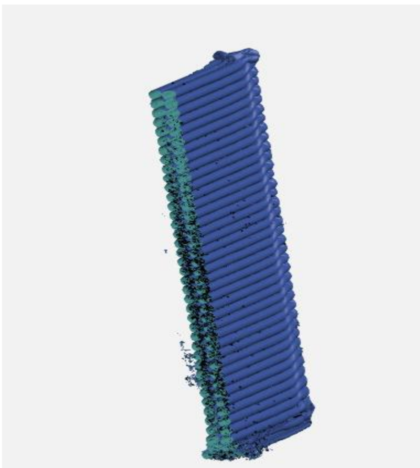

Figure 3.22- The cross-section of the specimen with no NBD shift in GOM Inspect

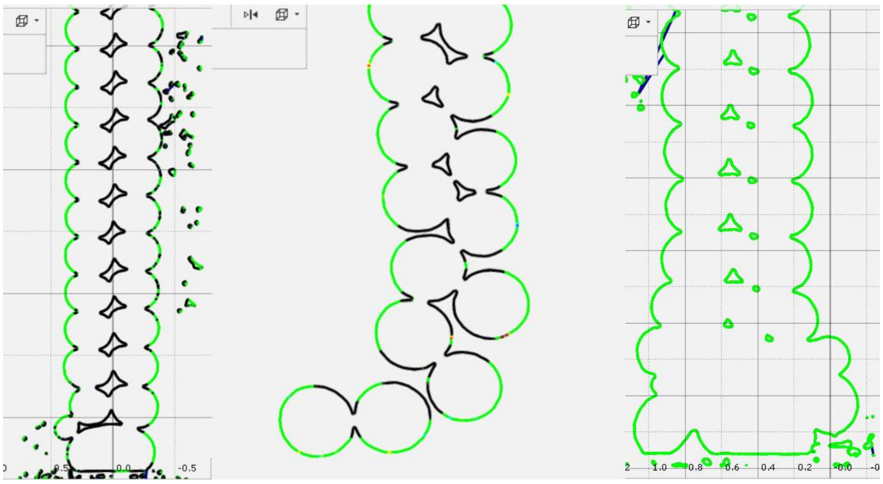

Figure 3.23- The geometry of bottom layers' cross-sections with: a) no NBD shift; b) +0.8 shift; c)-0.3 shift

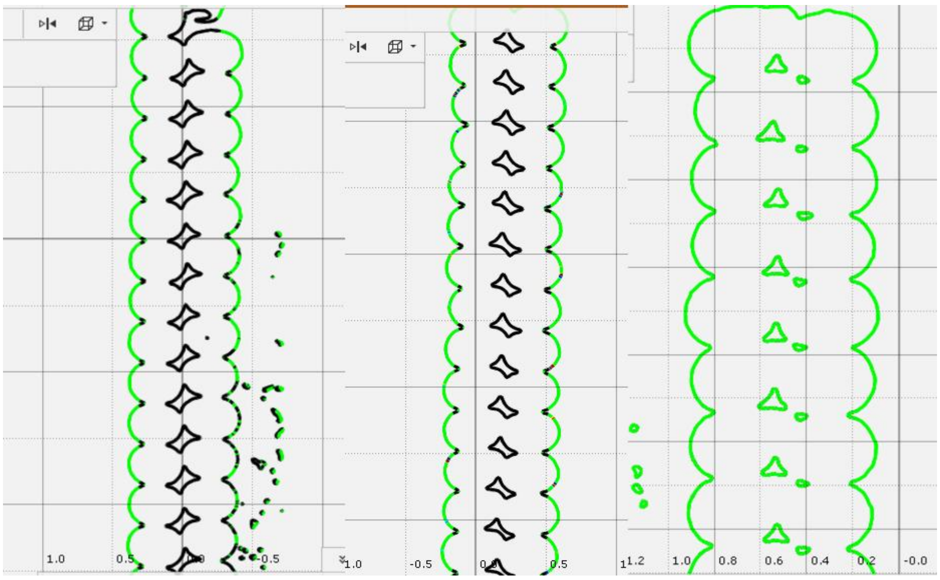

Figure 3.24- The geometry of top layers' cross-sections with: a) no NBD shift; b) +0.8 shift; c)-0.3 shift

As shown in Figure 3.23, for all NBD shift used, voids presented in all samples. These voids are mainly the gaps between the filaments deposited during printing. When the NBD shift is -0.3mm, the semi-molten filaments were closely deposited on the building platform, and there are no air gaps observed between the filaments in the first layer. The well-bonded first layer can reducing the heat loss from the second layer to the printing bed, which ensures the well-bonding of the filament in the following layers. As we can see from Fig.3.24, the voids of -0.3

mm samples are smaller than that of +0.8 mm NBD shift samples. The bad-bonded first layer accelerated the heat transfer to the platform and environment [6]. As a result, the sintering area between filaments decreases and voids or gaps between the beads were created in the next few layers. The formed void is large. However, when the NBD shift is higher (+0.8 mm), it can be seen that not every layer of adjacent filaments bonds have the same size necks (Fig.3.24). Actually, several layers near the bottom of the sample build thin sintering necks. By comparing these results, around five layers are influenced at large NBD shift, which is assumed to be the local variations in temperature as well as differences in localized cooling rates [28] induced by NBD shift.

The lengths of intra-bond lines and inter-bond lines were measured for different NBD shift. The results of measurements list in Table 3.12.

Table.3.12- The measurements of intra-bond lines length, inter-bond earlier and inter-bond later lines length for different NBD shift

NBD shift		intra bond	inter bond later	inter bond earlier
0	Mean, µm	118	169	168
	Std, µm	8	15	11
-0,3	Mean, µm	202	217	184
	Std, µm	6	33	13
0,8	Mean, µm	150	198	169
	Std, µm	30	31	28

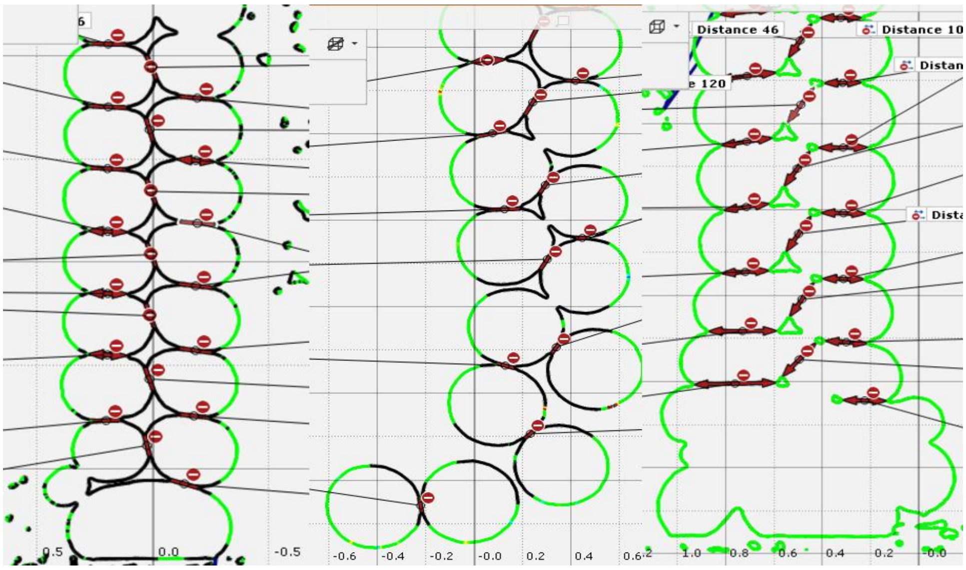

Figure 3.25- The intra- and inter-bond lines with: a) no NBD shift; b) +0.8 shift; c) -0.3 shift

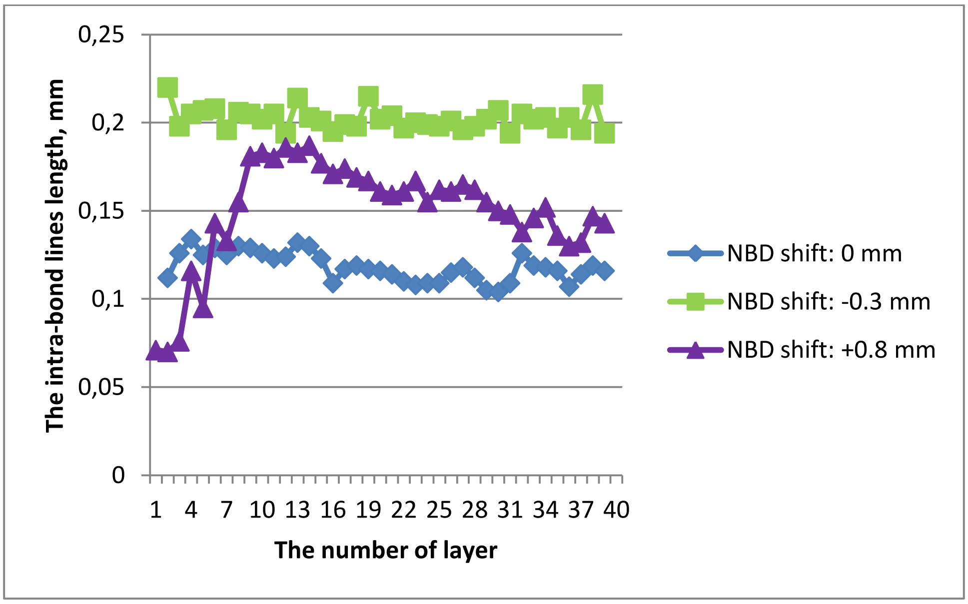

Figure 3.26- The graph of intra-bond lines length for different NBD shift

It was obtained that adhesion between and inside layers was better when NBD shift was -0.3 mm. This is reasonable. The explanation was considered above. There are some task about curves behavior for NBD shift: 0.8 mm. It was observed that adhesion in the sample was printed with +0.8 mm NBD shift is better than with no NBD shift. Though, it assumed a big gap between the first and second layers and therefore losing the heat. It can be seen in Fig.3.26 that the curve for

NBD shift +0.8 mm at the first several layers was below the curve for NBD shift 0 mm, but then it increased rapidly.

It is relative to the distance from the nozzle to the top of previous layer. The first layer was not changed for better adhesion with the bed. After the first layer there was a big gap (+1.1 mm from the top of the first layer) and the second layer was printed at this distance.

As were mentioned earlier half of the heat was transferred to the environment and printing platform. The adhesion between such layers is weak and as shown in Fig.3.24 the shape of bead is circular instead of elliptic as for NBD shift 0 mm. As a result the height of the layer is bigger in comparison with setting layer height (0.3 mm). It has visible effect on the first six layers.

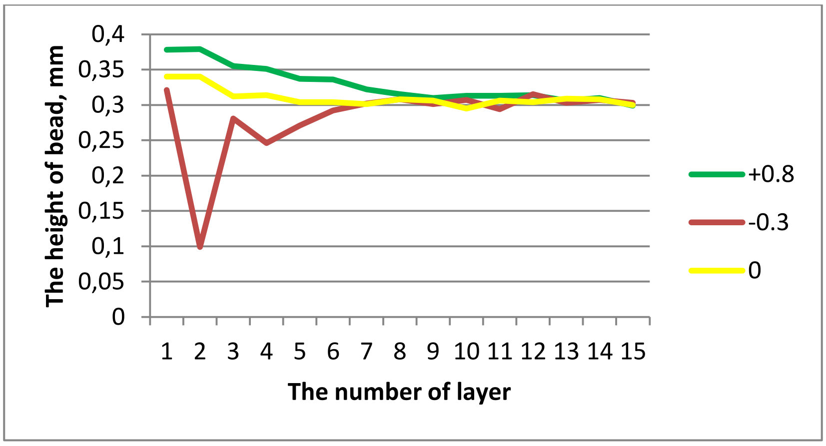

Figure 3.27- The actual height of the first 15 beads for different NBD shift

The measurement of height of the first 15 beads lists in Table 3.13 and shown in Fig.3.27. It leads to approaching of the nozzle to the top of layer with every layer and therefore it is occurred elliptical shape of a bead and the most adhesion when the nozzle is too close to the top of the previous layer (Fig.3.28). This was the reason why there was such conglutination from 8 till 14 layers (Fig.3.29).Then this process will stabilize if no changes are made again. This is also an explanation of the curve behavior for NBD shift +0.8 mm in Fig.3.26.

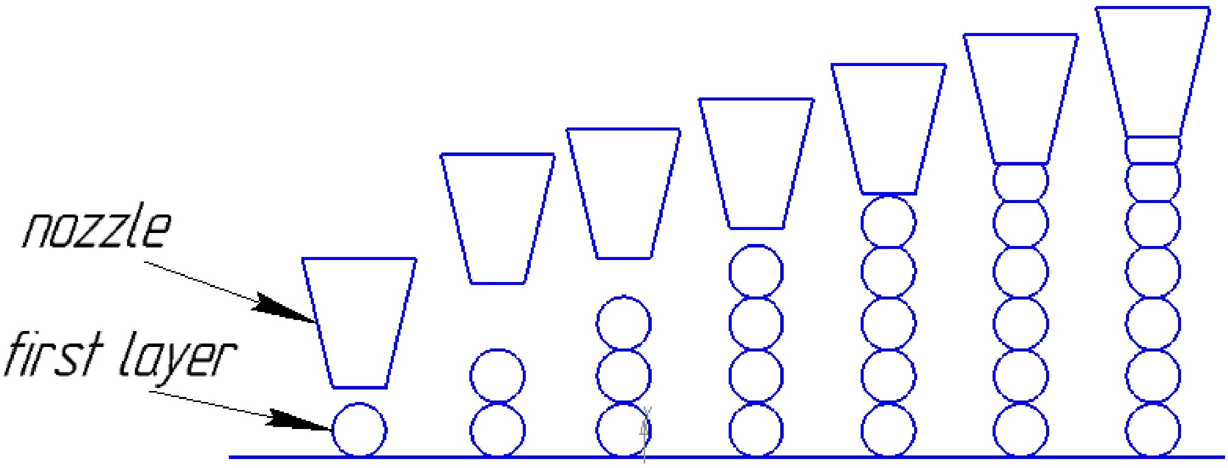

Figure 3.28- The scheme of printing nozzle movement for NBD shift: 0.8 mm

Table 3.13- The obtained height of the first 15 beads for different NBD shift

NBD shift, µm	0,8	-0,3	0
each layer			
1	378	321	340
2	379	99	340
3	355	281	312
4	351	246	314
5	337	271	304
6	336	292	304
7	322	302	301
8	315	308	308
9	310	301	306
10	313	307	295
11	313	294	306
12	314	315	304
13	306	303	309
14	310	307	308
15	299	303	300

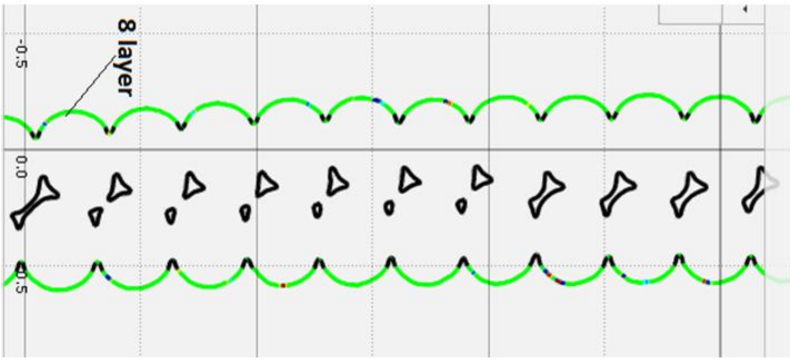

Figure 3.29- The 8-14 layers influenced by nozzle position

4 THE LABOUR PROTECTION AND SAFETY IN EMERGENCIES

4.1 Analysis of potential dangers

Work and researches that is executed in master's degree work envisage carrying out tests in the laboratory of additive manufacturing on the territory of campus De Nayer of Catholic university of Leuven, Belgium. And also experiment with resin embedment, polishing of samples and investigation under a microscope were conducted. For the removal of risks of traumatism, accidents and creation of the rationed terms of work it is necessary to adhere to the rules of accident prevention during work. Such dangerous and harmful factors on a researcher influence as:

- possibility to get burns from molten thermoplastics, or other steam-disengaging elements of device, the temperature of that can be varied from 170 to 300°C;
- an electrical shock as a result of abuse of safety rules during work with electric devices, violation of isolation of wires, disrepair of electric devices;
- the mechanical injuring in the consequence of not rational location of workplace, or due to insufficient attention of worker;
- the harmful evaporation of molten filament, that is distinguished during printing, contributing to the occurrence of pulmonary diseases, decline of immunity and allergic reaction;
- increased vibration and noise that is created with vibrations from 3D printers and PCs cause headache and fatigue in humans;
- working without special clothing can be result of contact with epoxy resin that can lead to health problems such as dermatitis and chemical burns;
- inhalation of highly concentrated epoxy resin vapors may cause irritation of the respiratory system in the absence of effective local ventilation;

- dust, abrasive grains, debris are a danger to the eyes when grinding without cooling and protecting agents;
- low skills of the employee may cause injury when working with a manual grinding machine;
- increased load on the organs of vision when working with a microscope;
- insufficient artificial and natural light levels can lead to rapid fatigue, impaired performance, myopia (acceptable levels of illumination in the area of a computer and small parts of 300-500 lux);
- intellectual overload can lead to fatigue, increased emotional state, sleep disturbance;
- increased pulsation of the light flux (with a pulsation coefficient of more than 5%) can lead to fatigue of the organs of vision, reduced attention, inhibition of brain activity, impaired vision;
- negative effects of your computer monitor, such as image fluctuation, brightness or darkness, and incorrect positioning of the monitor, all of these cause poor vision;
- the open frame of the printer may also cause the materials near the printer to catch fire;
- device malfunctions, such as a broken printer temperature sensor, can cause self-ignition (PLA).

4.2 Human safety measures

According to RLALP 0.00-4.12-05 "Typical provision on the procedure of conducting training and testing of knowledge on labor protection" the student undergoes an introductory labor protection briefing before beginning his research work. Also immediately prior to work in the workplace the direct supervisor conducts initial briefing.

To protect against possible burns and injuries related to molten plastic and epoxy resin, the worker is provided with personal protective equipment (special clothing, hand protection, eye protection) in accordance with NSU 7238: 2011 “SSWS. Means of collective protection of employees. General requirements and classification ” and RLALP 0.00-4.01-08“ Regulations on the procedure for providing workers with special clothing, special footwear and other personal protective equipment ”.

The facility of the laboratory for the level of electrical safety refers to the room without high risk - it is a dry room with a non-conductive floor, humidity not higher than 75%, without dust or only with a non-conductive dust, air temperature up to 30 ° C, which does not allow simultaneous human contact to the frame of electrical installations and metal elements connected to the ground.

In order to avoid possible electric shock of the service personnel, in the work are provided:

- organizational measures (conduct of training on the rules of electrical safety, knowledge testing and certification of personnel for the second or third group on electrical safety, according to RLALP 0.00-4.12-05 "Typical provision on the procedure for training and testing of knowledge on labor protection");
- technical measures (considering that the power supply of electrical equipment of the premises from the PC is carried out from the AC mains voltage of 220 V and a frequency of 50 Hz, according to the requirements of "RAEI-2014", electrical equipment in a room with a PC is characterized as electrical installations up to 1000 V, so according to the requirements chapter 1.7 "RAEI" and SS 12.1.030-81 (2001) "SSWS. Electrical safety. Protective earthing, grounding", the value of the resistance of the contour of the protective grounding of the electrical equipment of the premises from the PC at any time of the year does not exceed - 4 Ohms).

In accordance with the requirements of Directive 90/270 EEC, the basic requirements for monitors, which strictly regulate the safe working conditions and health protection of persons working with computers, are fulfilled:

- the characters on the screen are clear and well distinguished;
- an image devoid of blinking;
- brightness and / or contrast are easily adjustable;
- the screens are free from glare and reflection;
- radiation is reduced to extremely small levels.

The system unit and printer should not be placed inside the desk or in any other enclosed area where air circulation is impaired.

Filters that clean the air before it leaves the 3D printer are used to prevent air pollution by harmful evaporation. An additional obstacle is also the enclosure of the device, which partially deters harmful vapors.

To prevent the effects of harmful factors when working on a PC and 3D printer, it is necessary to observe the mode of work and rest.

4.3 Nervous-emotional loads in performing intellectual work and remedies

Unlike physical labor, mental labor is accompanied by lower energy supplies, but this does not indicate its ease. The main working body during this kind of work is the brain. With intense intellectual activity, the brain's energy requirement increases and is 15-20% of the total amount of energy consumed in the body. In this case, the use of oxygen 100 g of the cerebral cortex is 5 times greater than the skeletal muscles of the same weight at maximum physical activity. During the mental work the analytical and synthetic functions of the central nervous system are significantly activated, the reception and processing of information, there are functional connections, new complexes of conditioned reflexes, the role of functions of attention, memory, load on visual and auditory analyzers increases.

The functional stress of the body during work can be characterized on two sides - energy and information. The first prevails in physical, the second in mental labor. Characteristics of work that requires intensive brain work in obtaining and analyzing information, physiologists call tension. Labor tension is a characteristic of the labor process, which reflects the load mainly on the central nervous system, organs of senses, emotional sphere of the employee.

The intensity of the labor process is assessed in accordance with the State Sanitary Norms and Rules "Hygienic Classification of Labor by Indicators of Hazard and Hazardous Factors of Industrial Environment, Severity and Tension of the Labor Process", approved by the order of the Ministry of Health of Ukraine dated April 8, 2014 No. 248. The main indicators of tensions are duration of focus or signal density, degree of risk to one's own life and the lives of others, or degree of responsibility for the lives of others, variability in working exclusively at night shift. Auxiliary indicators are considered only in case of exceeding regulatory values.

The indicators characterizing the intensity of work include: intellectual, sensory, emotional load, the degree of monotony of the load, the mode of operation.

Intellectual workloads - are used exclusively for the assessment of the professions of mental work. Long-term mental activity affects mental activity, may impair attention, memory, perception (increased frequency of errors). Significant mental tension can lead to tachycardia (increased heart rate), increased blood pressure, changes in the electrical activity of the heart muscle and brain, increased pulmonary ventilation and oxygen consumption. Such functional changes in the body during long-term action can cause the development of inhibitory processes in the central nervous system, weakening alertness and attention, the development of fatigue.

Ergonomic indicators of labor intensity:

- number of objects of simultaneous observation;
- duration of focused observation or time of active action (in% of total working time);
- the density of signals (announcements) for 1 hour;
- emotional tension;
- variability;
- tension of analyzer functions;
- the amount of RAM;
- intellectual tension;
- monotony and others.

The easiest to consider is mental work, in which there is no need to make a decision. Such working conditions are considered optimal. If the operator works and makes decisions within one instruction, then such working conditions are permissible. Strenuous adverse conditions include work that is involved in solving complex problems using known algorithms or working with several instructions. Creative activities that require complex tasks in the absence of a clear solution algorithm should be referred to as hard work.

Processing any information or performing a task without evaluating its results is less difficult, allowing it to be evaluated as optimal. However, if these actions are accompanied by the need to verify the result obtained, then such working conditions are acceptable. Working on the division of production tasks between others and controlling their work are hard work.

The monotony of the performed operations leads to a certain condition of the person, called a monotomy. A sign of monotony is either an overload of the same information or a lack of new information. This imprints on the functional state of the person: she loses interest in the work being done. For her, working time seems to have stopped, and then she looks forward to the end of the shift, dropping her to sleep. Monotonous work reduces labor efficiency, increases staff turnover, accident rates and, as a consequence, injuries at work.

Prolonged work in conditions of constant nervous-emotional tension can lead to cardiovascular diseases. Any action that exceeds the permissible limits causes disturbance of the analyzer activity and even leads to pain. The task of the developers of technological processes - to prevent the overstress of higher nervous activity, otherwise stress can occur. Stress occurs in extreme situations when the body cannot adapt to emergency operations. The production process must be organized in such a way as to avoid stress. Occurrence of stress in an emergency situation causes the operator to act incorrectly, which often aggravates the production situation. An effective means of preventing stress in extreme conditions is professional training simulating emergencies.

Among the factors of increasing labor efficiency, a special place belongs to the rational mode of work and rest. Its structure depends on the dynamics of fatigue, the restoration of the body's functions, health and efficiency, reliability and productivity. Under the regime of work and rest means the total duration of work during the day, week, month, year, frequency and duration of periods of labor activity and breaks in the process of this activity, the ratio and alternation of these periods. The mode of operation includes the characteristics of the labor process itself - the intensity or intensity, as well as the permissible duration of the harmful factors.

A rational, physiologically sound mode of work and rest must meet the following requirements:

- prevent early and excessive development of employee fatigue;
- promote the maintenance of high performance and optimal functional state of the body of workers during the shift;
- ensure high productivity;
- promote effective restoration of physiological functions during rest.

4.4 Measures to ensure occupational health and hygiene

Measures to ensure industrial hygiene and occupational hygiene for the premises (research laboratory, design bureau, office, etc.) of the equipped VDT PC have been developed in accordance with the requirements of the State Sanitary Norms and Rules "Hygienic classification of labor by indicators of harmfulness and danger of production environment factors of the labor process", MJU 06.05.2014, № 472/25249, SSRN in 3.3.2.007-98" State standard rules and norms of work with visual display terminals of electronic computers” and RLALP 0.00-7.15-18 “Worker safety and health requirements for working with screen devices”.

The feet should be placed on a special stand or horizontal floor, the hips in the horizontal plane, and the forearms vertically, the elbows should be at an angle of 70-90 ° to the vertical plane, the wrists should be bent relative to the vertical plane not more than 20 °. The height of the work surface of the table is 680-800mm, and the width is sufficient to allow operations to be performed within the reach of the hands. The monitor screen should be positioned to provide visual observation in the vertical plane at an angle of ± 30 ° from the line of sight of the employee.

To prevent dustiness and contamination of the room with dust and fumes of plastic, which melts during 3D printing, it is necessary to provide common inflow and exhaust ventilation systems, which must provide three times the air exchange and meet the requirements of SBN B.2.5-67: 2013 "Heating, ventilation and air-conditioning".

According to SSN 3.3.6.042-99 "State sanitary norms of microclimate parameters" the temperature of the premises where the workers perform their duties while sitting and do not need physical exertion should be 22-24 ° C, the relative humidity of the room 40-60% - in the cold and the warm season. Indoor climate is provided according to SBN B.2.5-67: 2013 "Heating, ventilation and air conditioning".

Vibration level impact assessment should be performed according to NSU ISO 2631-1: 2004 “Vibration and impact mechanical. Assessment of the impact of general vibration on humans. "

Providing requirements for sanitary facilities (according to SBN B.2.2-28: 2010 "Buildings and constructions. Administrative and residential buildings"). The area of the premises should be taken at the rate of not less than 6 m^2 per workplace, and the volume - 20 m^3.

Workers with PCs are subject to mandatory medical examinations. Periodic inspections should be conducted every two years. The main criteria for assessing the state of fitness for work are the state of the organs of vision, while also taking into account the state of the organism as a whole. Order of the Ministry of Health of Ukraine of May 21, 2007. No. 246 “On approval of the procedure of medical examination of employees of certain categories”.

Natural and artificial lighting should be used when performing work on the premises. The illumination value on the surface of the desktop in the area of PC placement should be 400 lux, according to DBN B.2.5.-28-2018 "Natural and artificial lighting", if these values cannot be provided by the system of general lighting, it is allowed to use local lighting. Artificial lighting should be combined, ie combined with local lighting. It is recommended to use white spectral composition fluorescent lamps as artificial light sources. Local lighting should not create glare on the surface of the screen and increase the screen brightness of more than 400 lux. The ripple ratio should not exceed 5%. Therefore, it is recommended to use luminaires with diffusers and mirrored screen screens or reflectors with high-frequency starting devices. Fluorescent lamps in the composition of luminaires in general illumination recommended in rooms up to 6 m. LL lamps have the following advantages: high light output (up to 75 lm / W), high light flux stability, up to 10,000 hours, high color rendering index. Disadvantages: high cost, must be serviced by specialists, have sophisticated starting equipment, possible noise and flicker, significant ripple in the single-phase connection scheme”.

The maximum time-to-transmitted noise level shall not exceed 65-70 dBA. In the development of departmental standards, the permissible noise levels for certain types of work activities should be set taking into account the severity and intensity of work according to SSN 3.3.6.037-99 "Sanitary standards for industrial noise, ultrasound and infrasound".

4.5 Fire safety measures

Measures for fire safety at work in laboratories equipped with PC with VDT are developed in accordance with the requirements of FSR A.01.001-2014 "Rules of fire safety in Ukraine".

In a laboratory equipped with a personal computer and other electronic equipment, class A fire (a fire accompanied by the burning of solid materials) and an E (combustion of electrical installations up to 1000V) according to NSU EN 2: 2014 "Classification of fires (EN 2: 1992, EN 2: 1992 / A1: 2004, IDT)».

In accordance with the requirements of NSU B B.1.1-36: 2016 "Determination of categories of premises, buildings and exterior installations by fire and fire hazard", it belongs to the category "D" of fire hazard - space in a room containing solid combustibles and materials. As the premises (research laboratory) equipped with VDT PC belong to the category "D" of fire hazard, therefore according to the requirements of SBN B.1.1-7: 2016 "Fire safety of construction objects. General Requirements » it has II degree of fire resistance.

In the event of a fire in the research laboratory equipped with a VDT PC for evacuation of personnel in accordance with the requirements of SBN B.1.1-7: 2016 “Fire safety of construction objects. General requirements » there are exits, on both sides of the premises, on one side, and on the other - entrance doors. According to item 2.29 (Table 2) BR 2.09.02-85 * "Industrial buildings", the distance from the farthest workplace to the nearest escape route is not limited.

According to the requirements of SBN B.2.5-56: 2014 Fire Protection Systems, a fire alarm and alarm system "Signal-VK6" is installed in the premises (research laboratory) of the equipped VDT PC. Which provides detection of thermal and smoke signs of the fire and the place of occurrence of the fire with accuracy to the location of the sensor. Also to stop combustion indoors powder extinguishers should be installed.

4.6 Emergency safety measures

Methods of protection against the influence of electromagnetic pulse on the elements of production.

Nuclear explosions in the atmosphere and higher layers give rise to powerful electromagnetic fields with wavelengths of 1 to 1000 m or more. These fields are called electromagnetic pulse (EMP) because of their short-lived existence. EMP occurs during a nuclear explosion in wartime, in peacetime - when a nuclear weapon is tested or nuclear accidents and disasters occur in the atmosphere and space.

The main cause of EMPs of less than 1 s duration is the interaction of gamma rays and neutrons with nuclear gas atoms, resulting in electrons being ejected (Compton effect) and randomly dispersed in the medium of positively charged gas atoms. Also important is the occurrence of asymmetries in the distribution of spatial electric charges associated with the peculiarities of gamma rays propagation and electron formation.

Gamma rays emitted from the explosion zone toward the surface of the earth are absorbed in the denser layers of the atmosphere, knocking out fast atoms from the air atoms, flying in the direction of the gamma rays at the speed of light, and the positive ions (residual atoms) remain in place. As a result of the separation and displacement of positive and negative charges in this region and in the explosion zone, as well as in the interaction of charges with the Earth's geomagnetic field, elementary and resultant EMP electric and magnetic fields are formed that reach the surface of the earth within a radius of several hundred kilometers. Strong transverse currents occur, and the appearance of a large "flat antenna" is formed, which emits a powerful EMP with a rise time of decent 10 not longer than 230 no; with a frequency band from 10 kHz to 100 MHz. Depending on the height of the nuclear explosion, the nature, intensity of the EMP and the range of its propagation change under the same conditions.

At ground and low air explosion, the impact of the EMP is observed several kilometers from the center of the explosion. During a nuclear explosion, a symmetrical generation source is generated at altitudes of 3 to 25 km, but the radius of propagation of EMP remains limited due to the strong absorption of gamma radiation in dense atmospheric layers.

The most striking effect is EMP, which occurs during exoatmospheric explosions (more than 40 km). As the explosion height increases, so does the EMP source region, reaching thousands of kilometers in diameter and 20-40 km thick. Thus, during an explosion at an altitude of 80 km, EMP will spread over an area of radius 960 km and during an explosion at an altitude of 160 km - at an area of 1400 km. The exoatmospheric EMP is characterized by a very small rise time (several hundred nanoseconds), a high electric field intensity (greater than 50 kV / min) and a magnetic field (about 130 A / min). Lightning discharge compared to EMP has a much higher rise and fall duration (5–300 IU), creates very powerful fields (about 100 kV / min), carries much more energy, but the frequency spectrum is about 10 MHz, whereas for EMP it is larger - 100 MHz. The peak EMP value can reach 50,000 V / min, which is equal to all the energy emitted in the radio frequency portion of the spectrum.

The striking effect of EMP is due to the occurrence of voltages and currents in conductors of various lengths, located in the air, ground.

EMPs capture the frequency spectrum from tens to hundreds of megahertz, that is, the range within which power, communication and radar installations operate.

The electromagnetic field generated by EMP reaches 50,000 V / m, while in radar it does not exceed 200 V / m, and in connection - 10 V / m.

The EMP may vary from tens to hundreds of kilovolts per meter of antenna, depending on the degree of asymmetry of the explosion, whereas the sensitivity of conventional UDC receivers is several tens or hundreds of microvolts. Thus, in the case of a 1Mt land explosion, the field strength at a distance of C km is about 50 kV / m, and at a distance of 16 km - 1 kV / m. And in the case of an atmospheric explosion of the same power, the field strength will be thousands of kilovolts per square meter in several thousand square kilometers of the earth's surface.

The rise time of the EMP to the maximum is a few billionths of a second, which is significantly less than the time of operation of known electronic protection systems. This means that when EMP arrives, sensitive electronic equipment will receive a very large overload, which it will not be able to withstand.

EMP parameters depend on the power and height of the explosion, as well as the distance from the epicenter of the explosion. In the case of explosions above the atmosphere at an altitude of more than 100 km of the megaton range, EMPs are created that cover a large area, many thousands of square kilometers.

EMP magnetic and electric fields are characterized by field strength. In dynamics, EMI impulse is a fast damping oscillatory process with several quasi-periods.

The striking effect of EMP on the ground and on the ground is related to the accumulation of its energy by long metallic objects, frame and frame structures, antennas, transmission lines and communications; in the area of EMP, direct contact of a person with conductive objects is dangerous.

EMP strikes radio electronic and radio equipment. High voltages and currents are induced in the conductors, which can lead to permanent or temporary damage to the cable insulation, switching off relays and circuit breakers, damage to communication elements, magnetic storage devices in computers and data transmission systems, etc. The most vulnerable components of the equipment are semiconductor devices - transistors, diodes, silicon rectifiers, integrating circuits, digital processors, control and control devices. EMP sensitive sound transistors, switching transistors, integrating circuits, etc.

Particularly sensitive to the effects of EMP are the 6 main groups of objects and systems:

a) power transmission systems: overhead transmission lines, cable lines, various types of connecting lines and overhead wiring;

b) systems of production, transformation and accumulation of energy: power plants, direct and alternating current generators, transformers, converters of currents and voltages, switches and switchgear, electric batteries and accumulators, fuel, solar and thermoelements;

c) systems of regulation and control: electromechanical and electronic sensors and other elements of automatics, computer installations;

d) electricity consumption systems: electric motors and electromagnetic, heating, refrigeration, ventilation, lighting installations and air conditioners;

e) electrical systems: electric drives, semiconductors and other types of converters;

f) systems of radio communication, transmission, storage and accumulation of information: antennas, waveguides, coaxial cables, electronic devices, radio transmitters, radios, installations of autonomous power supply, mixers, telephone sets, telegraph installations, grounded cables and wires, automatic telephone exchange.

The most EMP resistant vacuum electronic devices that fail at 1 J. The amount of EMP energy depends on the frequency bandwidth of the antenna systems.

Most communication systems operate in the mid to ultra high frequency range and will be damaged depending on the frequency range. Radar systems are less damaging to EMP because they operate in a frequency range where EMP energy density is low. Sparking caused by the high EMP electric field can cause gasoline vapors and other leaks to build up in storage.

If a nuclear explosion occurs near a power line, a long-range link, then the voltages indicated therein can spread over many kilometers of wires, damage the equipment, and strike people at a safe distance from other nuclear explosive factors.

EMP is dangerous even in the presence of solid structures designed to withstand a shock wave of a ground-based nuclear explosion conducted over several hundred meters.

The current level of knowledge about the nature and properties of EMP makes it possible to develop protection against it and to implement security measures that include electromagnetic interference circuits, electronic components resistant to EMP, shielding of individual devices or entire electronic systems.

The ideal protection against EMP would be full cover of the room, which houses the radio-electronic equipment, a metal screen.

At the same time, it is clear that it is practically impossible to provide such protection in some cases, because for the equipment to work it is often necessary to provide its electrical connection with external devices. Therefore, less reliable means of protection are used, such as conductive grids or film coverings for windows, cellular metal structures for air intakes and ventilation openings, and contact spring gaskets located around the perimeter of doors and hatches. A more difficult technical problem is protection against the penetration of EMP into the equipment through various cable entries. The radical solution to this problem could be the transition from electrical communication networks to practically not subject to the action of fiber optic EMP. However, the replacement of semiconductor devices in the entire spectrum of functions performed by electronic-optical devices is possible only in the distant future. Therefore, currently, as a means of protection of cable inputs, the most widely used filters, including fiber, as well as spark arresters, metal oxide varistors and high-speed Zener diodes.

All these tools have both advantages and disadvantages. Yes, capacitive inductive filters are quite effective for low-intensity EMP protection, and fiber filters protect in a relatively narrow range of ultra-high frequencies. Spark arresters have considerable inertia and are basically suitable for protection against overloads arising under the influence of voltages and currents induced in the skin of the aircraft, the casing of the equipment and the braid of the cable.

Metal oxide varistors, which are semiconductor devices, dramatically increase their conductivity at high voltage.

However, when using these devices as a means of protection against EMP, their low performance and deterioration in repeated loads should be taken into account. These disadvantages are absent in high-speed Zener diodes, whose action is based on a sharp avalanche resistance change from a relatively high value to almost zero when the applied voltage of a certain threshold value is exceeded. In addition, unlike varistors, the characteristics of the Zener diodes do not deteriorate after multiple high-voltage effects and mode switching. The most rational approach to the design of the EMP protection of cable glands is to create such connectors, in the design of which there are special measures to ensure the formation of filter elements and the installation of built-in Zener diodes. Such a solution helps to obtain very small capacitance and inductance values, which is necessary to provide protection against impulses that have low duration and therefore a powerful high-frequency component. Using connectors of this design will solve the problem by limiting the mass-dimensional characteristics of the protection device.

The complexity of solving the problem of protection against EMP and the high cost of tools and methods developed for these purposes make the first steam on the path of their selective use in particularly important systems of weapons and military equipment. The first targeted work in this direction was the EMP protection programs for strategic weapons. The same path is chosen and for protection they have a great length of control and communication systems. However, foreign experts consider the creation of so-called distributed communication networks (such as "Gwen"), the first elements of which are already deployed in the continental United States, as the main method of solving this problem.

CONCLUSIONS AND FUTURE WORK

In this work the influence of location on bond length was investigated. It was obtained that the plane characterized by the shortest intra-layer time presents the longest bond length. It was detected that in general length of inter-layer bond (late) are longer than inter-layer bond (early). This was explained with reference to the temperature profile during deposition.

The results of influence of printing speed on bonding formation showed that lengths of intra- and inter-layer bond lines are generally higher for 20 mm/s than for 10 mm/s.

The weighing of samples with different extrusion multiplier was made to obtain limit print speed. The results indicated that the machine can not print faster than 85.68 mm/s for certain printing parameters (layer height 0.3 mm; nozzle diameter 0.4 mm).

The effect of extrusion multiplier on parts thickness was observed. The thickness grows with increasing EM. Also the measurement results of influence EM on bond length was represented. If set above 1, it allows creating more dense prints, but too high values can sometimes cause material overflow the defined shape of printed element, resulting in lowering dimensional accuracy but stronger prints. In opposite case, with extrusion multiplier <1, the resulting print is created with less than optimal amount of filament, resulting in worse bonding.

The influence of NBD shift on cross-sectional profile was clarified in this work. It has significant effect on the several first layers, but then the process is stabilized. It was observed that adhesion in the sample was printed with +0.8 mm NBD shift is better than with no NBD shift. The features in cross-section at NBD shift +0.8 mm were considered.

The basic safety provisions for conducting these researches and the potential dangers of handling the equipment was considered.

The future work can be directed on researching of temperature profile during deposition under different printing parameters to confirm all data received from this work. Also the porosity and effect of combination of different parameters on cross-sectional profile can be investigated and these parameters can be applied for more complex geometry of a part.

REFERENCES

[1] Jose F. Rodriguez, James P. Thomas, and John E. Renaud, “Characterization of the mesostructure of fused deposition acrylonitrile butadiene styrene materials,” *Rapid Prototyp. J.*, vol. 6, no. 3, pp. 175–186, 2000.

[2] Q. Sun, G. M. Rizvi, C. T. Bellehumeur, and P. Gu, “Effect of processing conditions on the bonding quality of FDM polymer filaments,” *Rapid Prototyp. J.*, vol. 14, no. 2, pp. 72–80, 2008.

[3] C. Bellehumeur, L. Li, Q. Sun, and P. Gu, “Modeling of bond formation between polymer filaments in the fused deposition modeling process,” *J. Manuf. Process.*, 2004.

[4] H. Li, T. Wang, and Z. Yu, “The Quantitative Research of Interaction between Key Parameters and the Effects on Mechanical Property in FDM,” *Adv. Mater. Sci. Eng.*, 2017.

[5] S. F. Costa, F. M. Duarte, and J. A. Covas, “Thermal conditions affecting heat transfer in FDM/FFE: a contribution towards the numerical modelling of the process: This paper investigates convection, conduction and radiation phenomena in the filament deposition process,” *Virtual Phys. Prototyp.*, vol. 10, no. 1, pp. 35–46, 2015.

[6] S. F. Costa, F. M. Duarte, and J. A. Covas, “Estimation of filament temperature and adhesion development in fused deposition techniques,” *J. Mater. Process. Technol.*, vol. 245, pp. 167–179, 2017.

[7] L. Li, Q. Sun, C. Bellehumeur, and P. Gu, “Composite modeling and analysis for fabrication of FDM prototypes with locally controlled properties,” *J. Manuf. Process.*, vol. 4, no. 2, pp. 129–141, 2002.

[8] O. A. Mohamed, S. H. Masood, and J. L. Bhowmik, “Optimization of fused deposition modeling process parameters: a review of current research and future prospects,” *Adv. Manuf.*, 2015.

[9] M. P. Serdeczny, R. Comminal, D. B. Pedersen, and J. Spangenberg,

"Experimental validation of a numerical model for the strand shape in material extrusion additive manufacturing," *Addit. Manuf.*, vol. 24, no. September, pp. 145–153, 2018.

[10] B. N. Turner and S. A. Gold, "A review of melt extrusion additive manufacturing processes: II. Materials, dimensional accuracy, and surface roughness," *Rapid Prototyp. J.*, vol. 21, no. 3, pp. 250–261, 2015.

[11] B. N. Turner, R. Strong, and S. A. Gold, "A review of melt extrusion additive manufacturing processes: I. Process design and modeling," *Rapid Prototyp. J.*, vol. 20, no. 3, pp. 192–204, 2014.

[12] W. ASSOCIATES, "Executive summary of the Wohlers Report 2016," p. 12, 2016.

[13] H. Bikas, P. Stavropoulos, and G. Chryssolouris, "Additive manufacturing methods and modeling approaches: A critical review," *Int. J. Adv. Manuf. Technol.*, 2016.

[14] C. Ziemian, M. Sharma, and S. Ziemi, "Anisotropic Mechanical Properties of ABS Parts Fabricated by Fused Deposition Modelling," *Mech. Eng.*, 2012.

[15] A. Boschetto and L. Bottini, "Accuracy prediction in fused deposition modeling," *Int. J. Adv. Manuf. Technol.*, 2014.

[16] M. Taufik and P. K. Jain, "A Study of Build Edge Profile for Prediction of Surface Roughness in Fused Deposition Modeling," *J. Manuf. Sci. Eng.*, 2015.

[17] R. Anitha, S. Arunachalam, and P. Radhakrishnan, "Critical parameters influencing the quality of prototypes in fused deposition modelling," in *Journal of Materials Processing Technology*, 2001.

[18] K. G. J. Christiyan, U. Chandrasekhar, and K. Venkateswarlu, "A study on the influence of process parameters on the Mechanical Properties of 3D printed ABS composite," in *IOP Conference Series: Materials Science and Engineering*, 2016.

[19] A. K. Sood, R. K. Ohdar, and S. S. Mahapatra, "Parametric appraisal of mechanical property of fused deposition modelling processed parts," *Mater.*

Des., 2010.

[20] M. Spoerk, F. Arbeiter, H. Cajner, J. Sapkota, and C. Holzer, “Parametric optimization of intra- and inter-layer strengths in parts produced by extrusion-based additive manufacturing of poly(lactic acid),” *J. Appl. Polym. Sci.*, vol. 134, no. 41, pp. 1–15, 2017.

[21] P. Ravi, P. S. Shiakolas, and A. Dnyaneshwar Thorat, “Analyzing the Effects of Temperature, Nozzle-Bed Distance, and Their Interactions on the Width of Fused Deposition Modeled Struts Using Statistical Techniques Toward Precision Scaffold Fabrication,” *J. Manuf. Sci. Eng.*, 2017.

[22] J. M. Chacón, M. A. Caminero, E. García-Plaza, and P. J. Núñez, “Additive manufacturing of PLA structures using fused deposition modelling: Effect of process parameters on mechanical properties and their optimal selection,” *Mater. Des.*, vol. 124, pp. 143–157, 2017.

[23] R. Comminal, M. P. Serdeczny, D. B. Pedersen, and J. Spangenberg, “Numerical modeling of the strand deposition flow in extrusion-based additive manufacturing,” *Addit. Manuf.*, vol. 20, pp. 68–76, 2018.

[24] NatureWorks, “Ingeo ™ Biopolymer 3D850 Technical Data Sheet 3D Printing Monofilament – General Purpose Grade,” no. 4, pp. 1–4.

[25] E. Ferraris, J. Zhang, and B. Van Hooreweder, “Thermography based in-process monitoring of Fused Filament Fabrication of polymeric parts,” *CIRP Ann. - Manuf. Technol.*, vol. 3, p. (in press), 2019.

[26] B. Wittbrodt and J. M. Pearce, “The effects of PLA color on material properties of 3-D printed components,” *Addit. Manuf.*, vol. 8, pp. 110–116, 2015.

[27] C. Aydemir, S. Yenidoğan, A. Karademir, and E. Arman, “Effects of color mixing components on offset ink and printing process,” *Mater. Manuf. Process.*, vol. 32, no. 11, pp. 1310–1315, 2017.

[28] C. Koch, L. Van Hulle, and N. Rudolph, “Investigation of mechanical anisotropy of the fused filament fabrication process via customized tool path generation,” *Addit. Manuf.*, 2017.

Variations of cross sectional profile geometry of extruded strand in fused filament fabrication (FFF)

Supervisor: associate professor Eduard Kondratiuk

Student: Larysa Hurina

Engineering Technology Department

Content

1. Context and problem statement
2. Objectives
3. Materials and methods
4. Experimental results and discussion
5. Conclusion

1. Context and problem statement

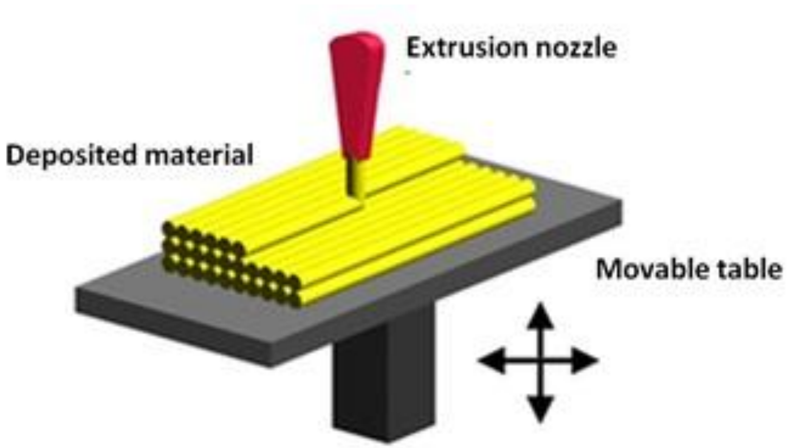

FFF process

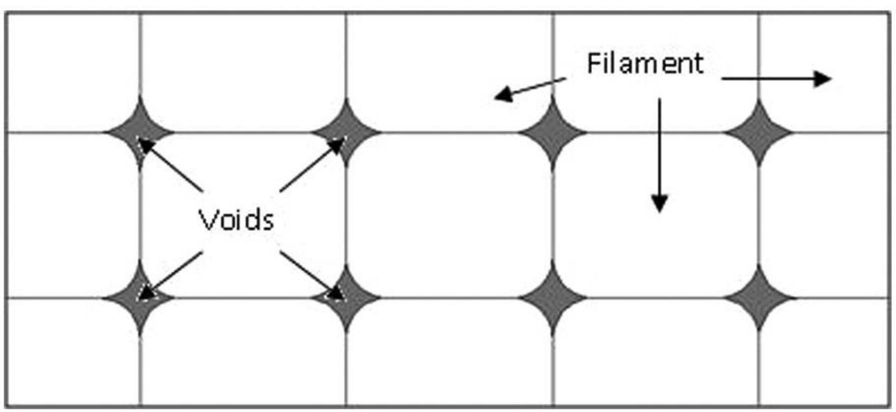

Mesostructure of FFF parts

(Picture credits to B. Huang and S. Singamneni, Proc. Inst. Mech. Eng. Part B J. Eng. Manuf.,vol.228, no. 1, pp. 111–126, 2014.)

- Semi-liquid material is extruded through a nozzle and selectively deposited in the form of a strand.
- The extruded strands bond to the previously deposited material by temperature-driven diffusion process.
- This process determines the cross-section of FFF parts.

1. Context and problem statement

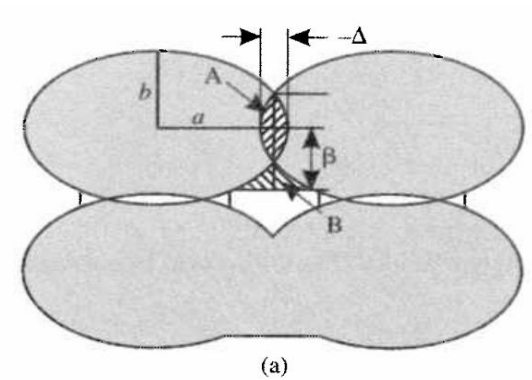

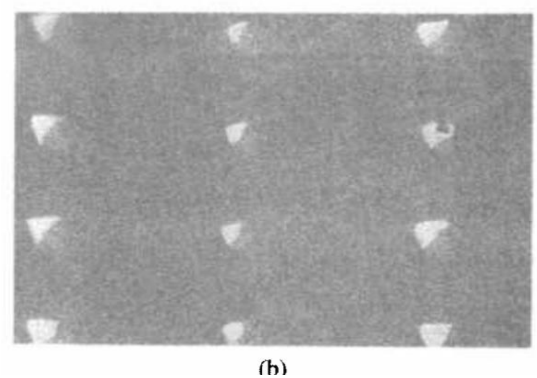

(Pictures credit to L. Li, et al "Composite modeling and analysis for fabrication of FDM prototypes with locally controlled properties," *J. Manuf. Process.*, vol. 4, no. 2, pp. 129–141, 2002)

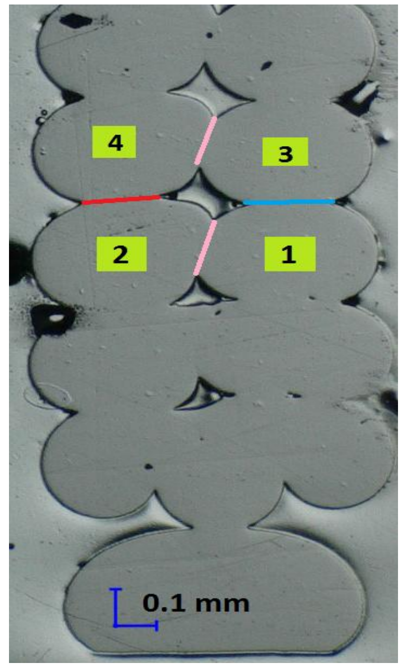

Cross-section of the sample under microscopy

- The cross-section profile describes shape of the strands, bond lines, porosity.

Pink- intra-layer bond lines (within layers)
Blue- inter-layer bond line (early)(between layers)
Red- inter-layer bond line (late)(between layers)

1. Context and problem statement

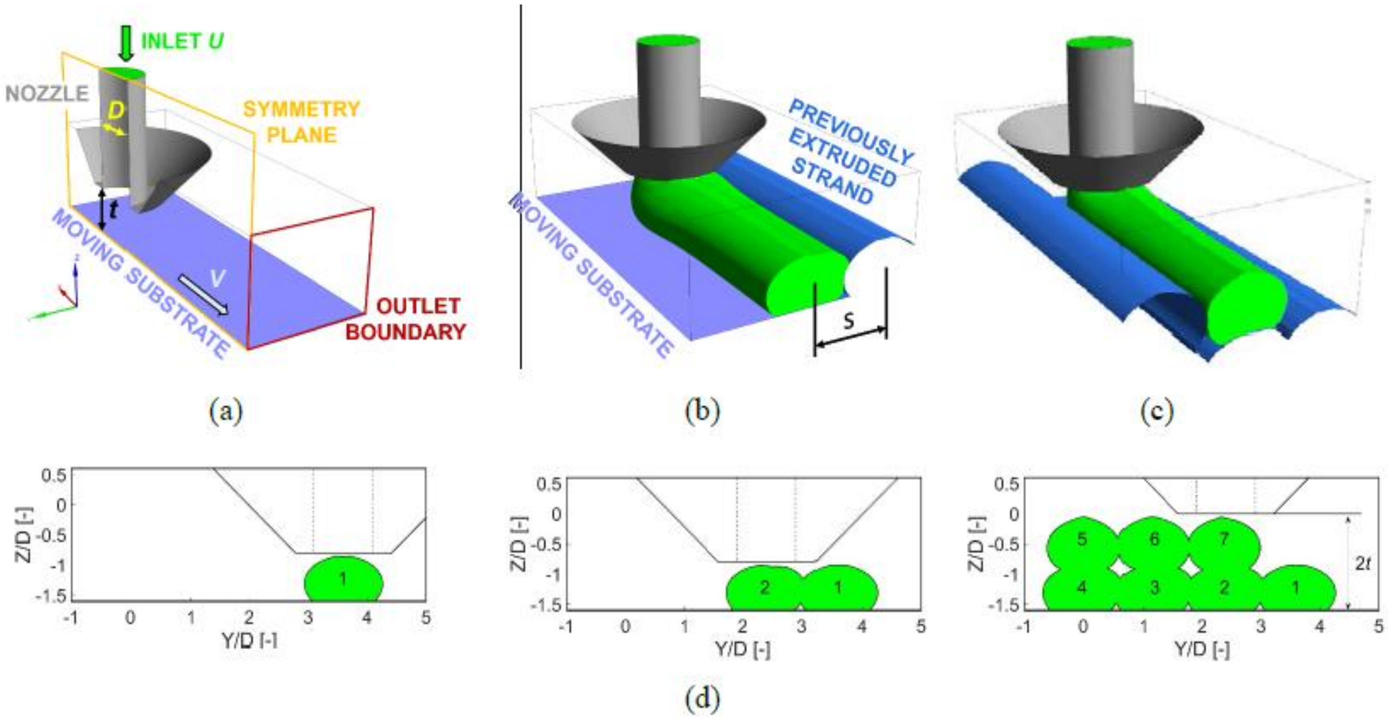

(Pictures credit to M. P.Serdeczny, et al, "Numerical Prediction of the Porosity of Parts Fabricated with Fused Deposition Modeling," pp. 1849–1854, 2018)

Numerical model of strand deposition

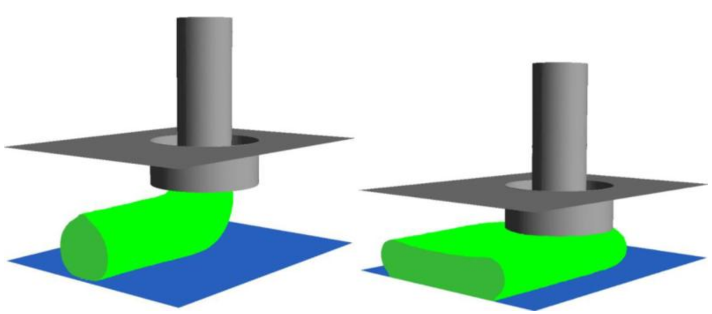

•Decreasing the layer height deforms the strand and changes its shape from an oval (for a large layer height), to a flat cuboid with rounded corners (for a small layer height).

1. Context and problem statement

•FFF parts have a smaller tensile strength than components fabricated with conventional manufacturing techniques.

•A mesostructure with large voids results in a small contact area between the strands and poor bonding.

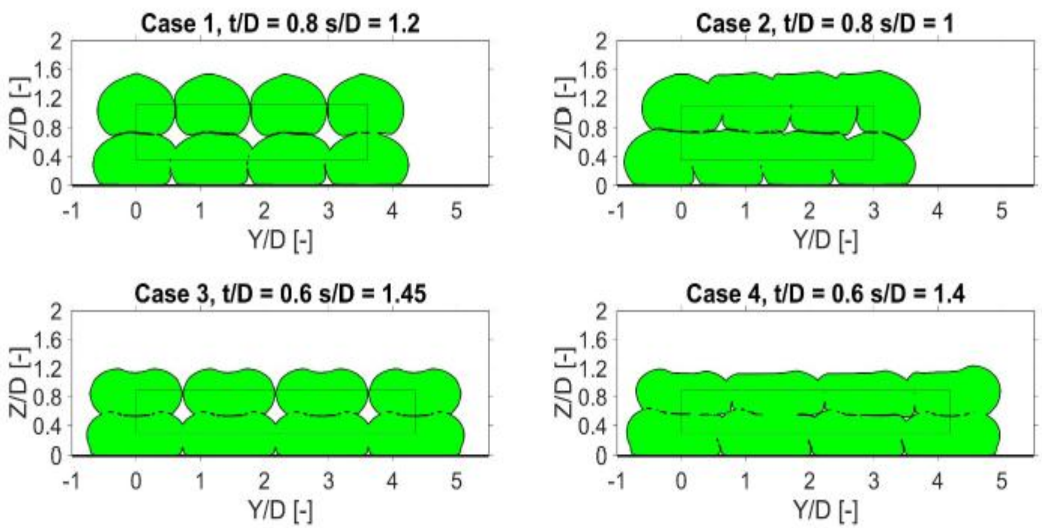

•Cross-sections of the simulated strands, extruded at different normalized layer thicknesses *t/D and*
normalized strand-to-strand distances *s/D.*

	Case 1	Case 2	Case 3	Case 4
Normalized layer thickness	0.8	0.8	0.6	0.6
Normalized strand-to-strand distance	1.2	1	1.45	1.4
Porosity	0.100	0.045	0.074	0.015

(Pictures credit to M. P.Serdeczny, et al, “Numerical Prediction of the Porosity of Parts Fabricated with Fused Deposition Modeling,” pp. 1849–1854, 2018)

2.Objectives

- The goal is to investigate the influence of printing conditions on the cross-section geometry of the deposited strands and bonding between them.

  Investigated parameters:

- ➢ Nozzle-bed distance
- ➢ Feed rate
- ➢ Printing speed

3. Materials and methods

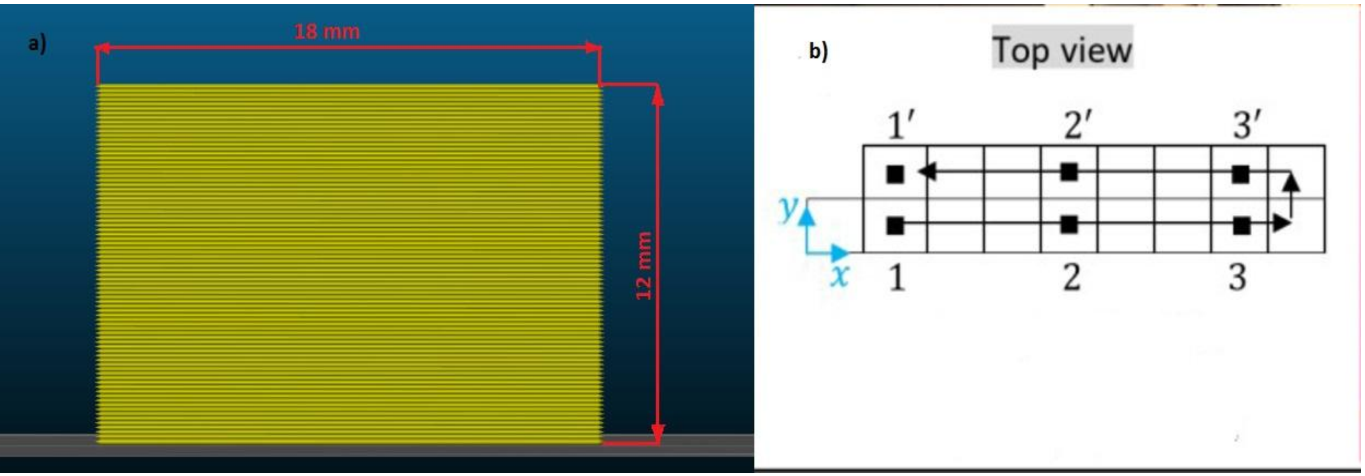

Samples geometry and sequence of deposition

3D-printer Prusa i3 MK3

Printing parameters

Parameters	Values
Model dimension $L \times W \times H$	$18 \times 0.8 \times 12$ mm^3
Layer thickness Δh	0.3mm
Printing speed v	20 mm/s, 10 mm/s
Nozzle temperature T_n (nominal)	215 °C
Platform temperature T_p (nominal)	60°C
Air temperature T_a	21°C
Fan speed	On- max speed
Nozzle diameter (E3D V6 nozzle type)	0.4 mm
PLA filament diameter (PRUSA supplier)	1.75 mm

Properties of material

Properties	PLA
Tensile strength	60 MPa
Elongation	6%
Flexural modulus	3.8 GPa
Density	1.23 -1.25 g/cm^3
Melting point	145-160°C
Glass transition temperature	55-60°C
Biodegradable	Yes, under the correct conditions

3. Materials and methods

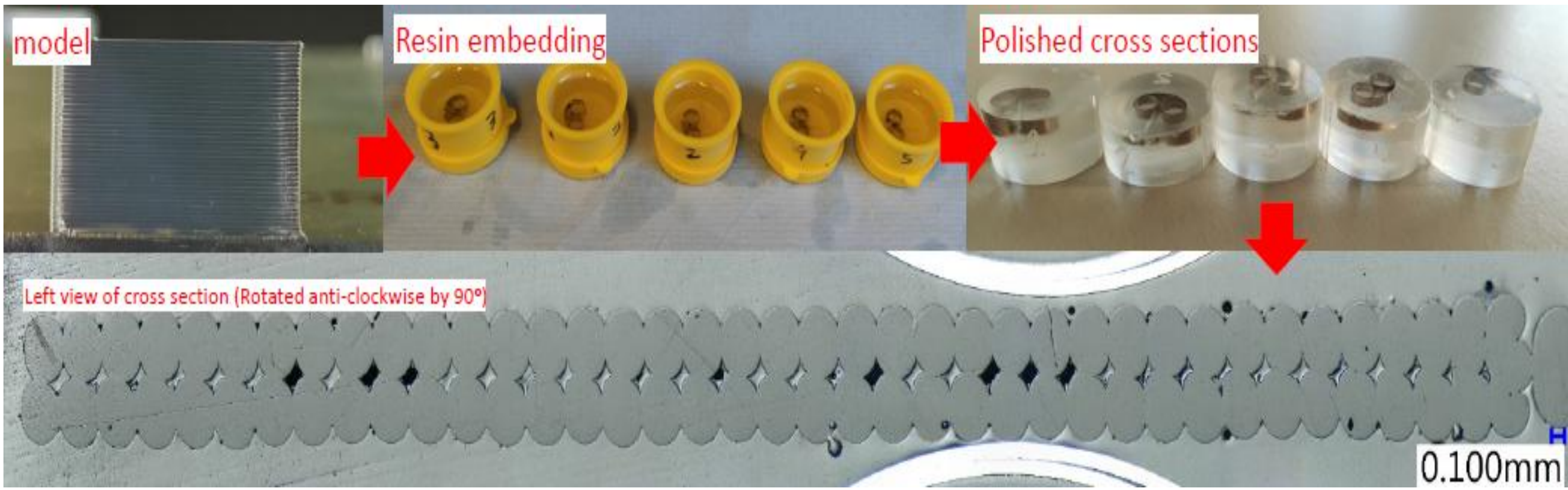

Resin embedment of cut sample,
polishing and observing of cross-section
under optical microscopy

3. Materials and methods

•Nikon XT H225ST: focal spot size 8 µm, resolution 11-15µm;

Computed tomography scanner

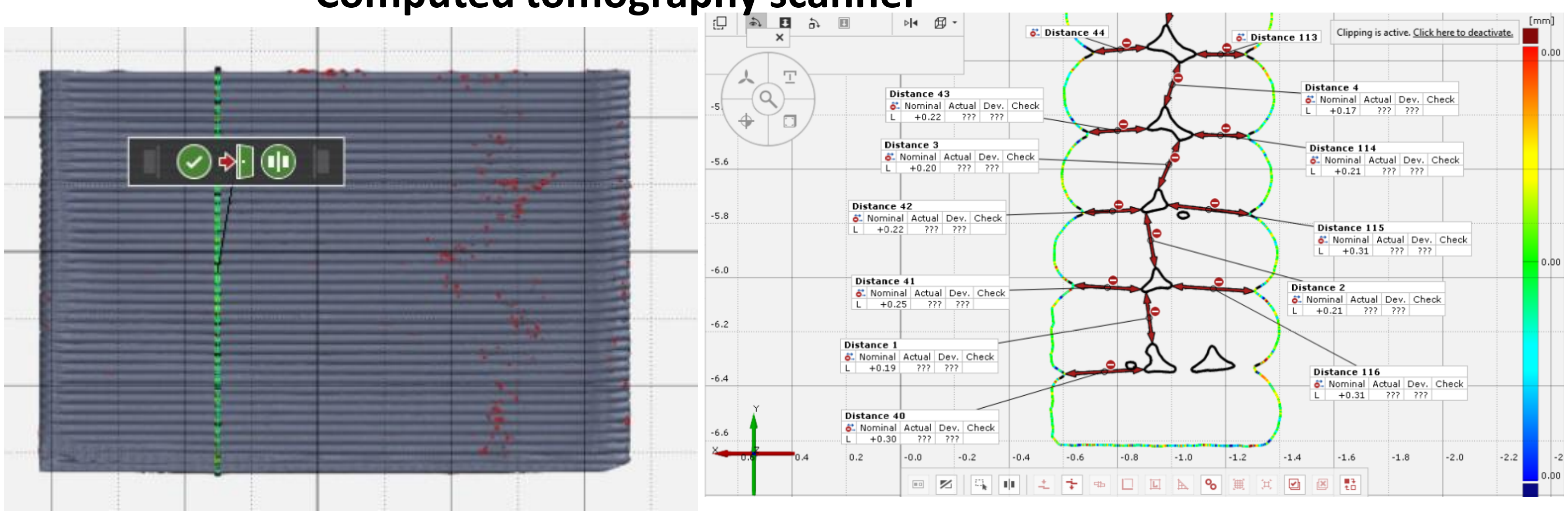

Data analyze in GOM Inspect software

4.Experimental results and discussion

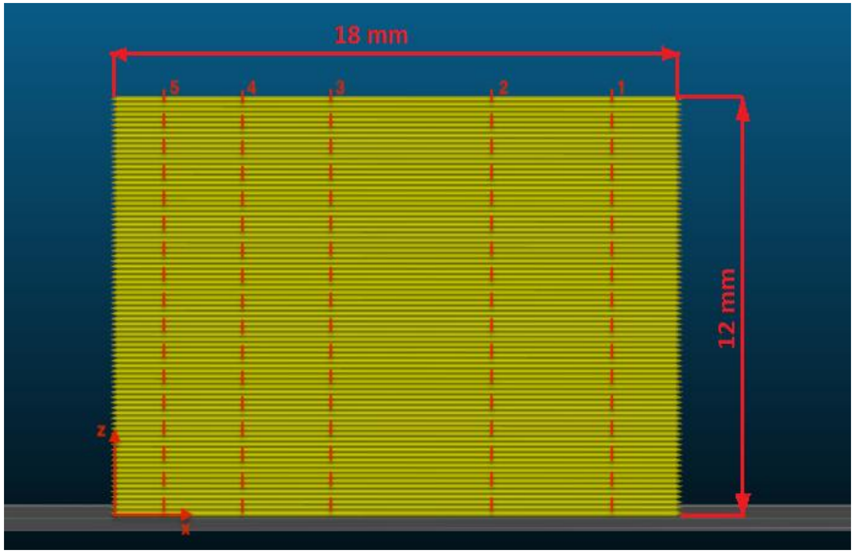

Location of cross-sections

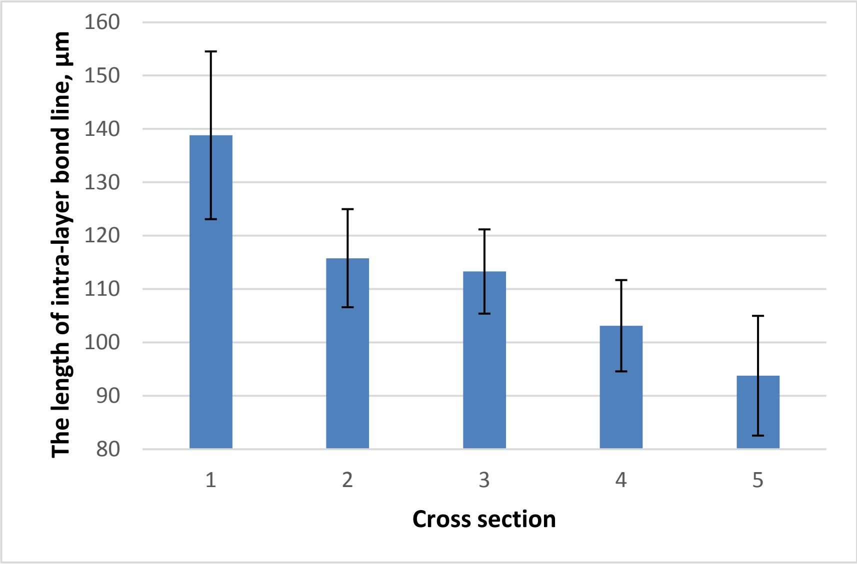

The length of intra-layer bond lines at 5 sections

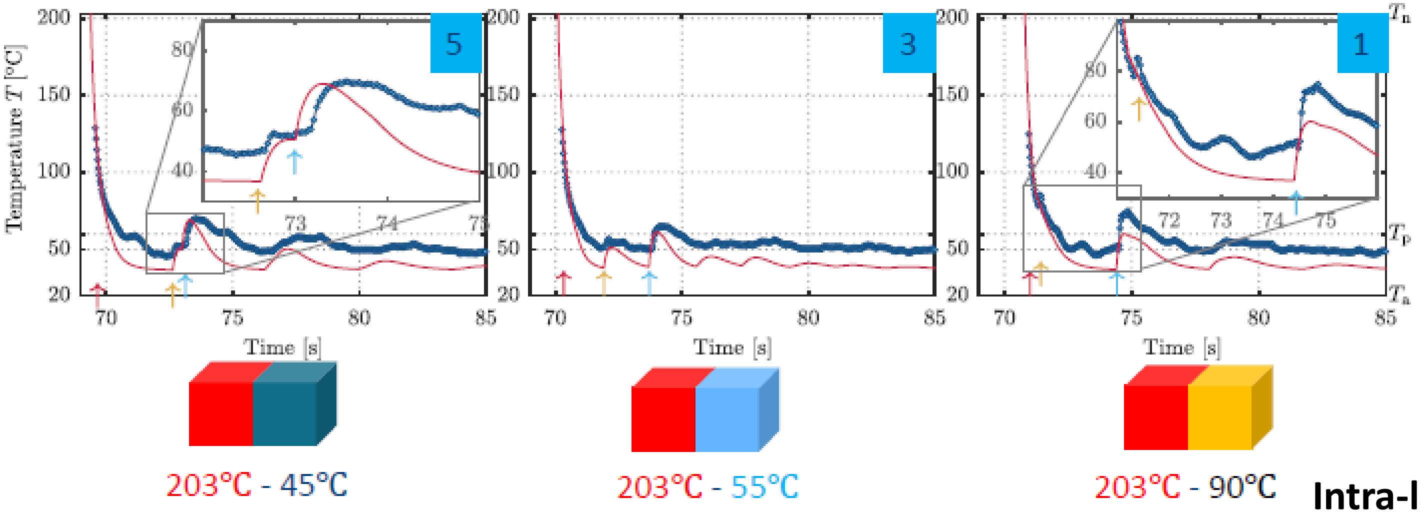

Temperature profile of filaments at cross-sections 1, 3, 5

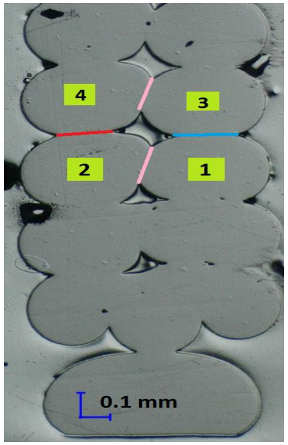

Intra-layer bond line- pink lines

4.Experimental results and discussion

- In general the lengths of inter-layer bond lines(late) are longer than inter-layer bond lines (early);
- The sequence of deposition and heat transfer between environment and filaments must be taken into account.

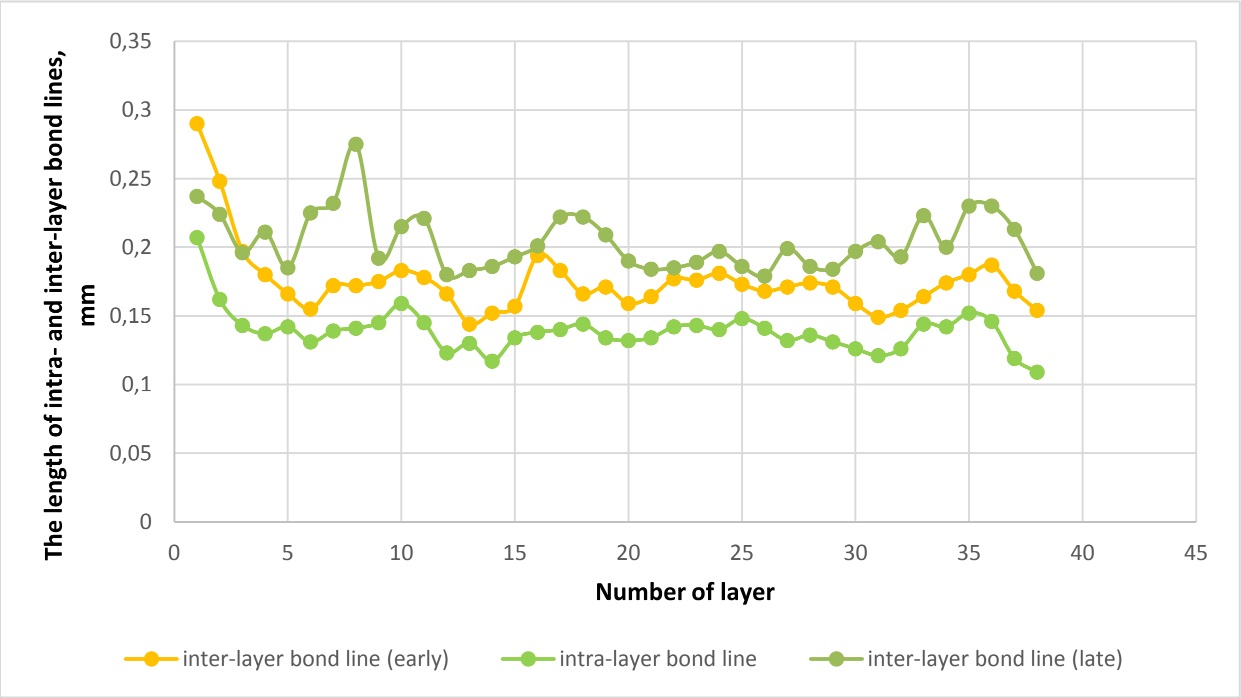

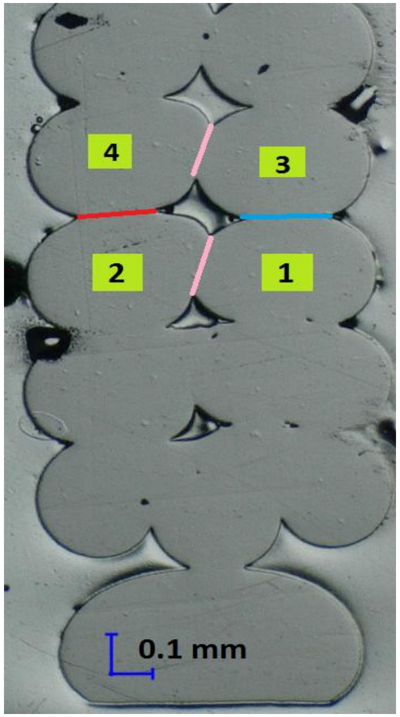

The length of intra- and inter-layer bond lines

Inter-layer bond line (early)- blue line
Inter-layer bond line (late)- red line.

4.Experimental results and discussion

- Computed tomography scanning results (CT)

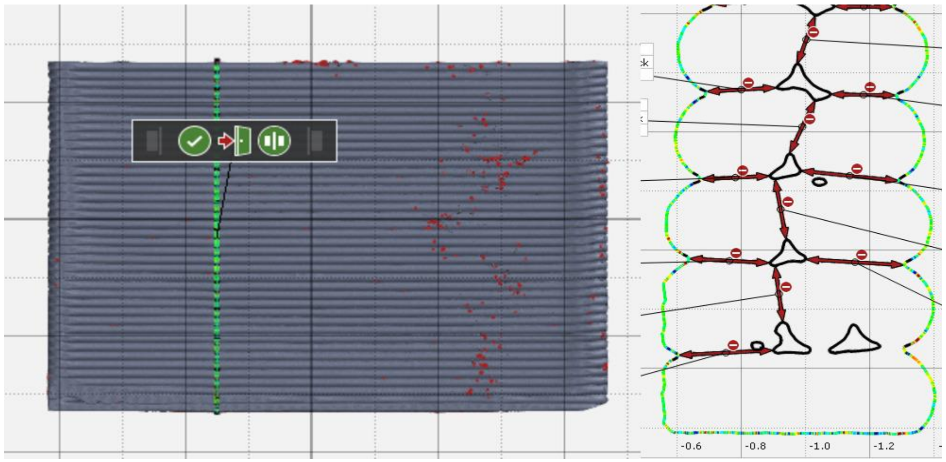

Cross-section in GOM Inspect

Location of cross-sections in GOM Inspect

cross-section	X coordinate
1	16.3 mm
2	12.3 mm
3	9.7 mm
4	6.3 mm
5	2.7 mm

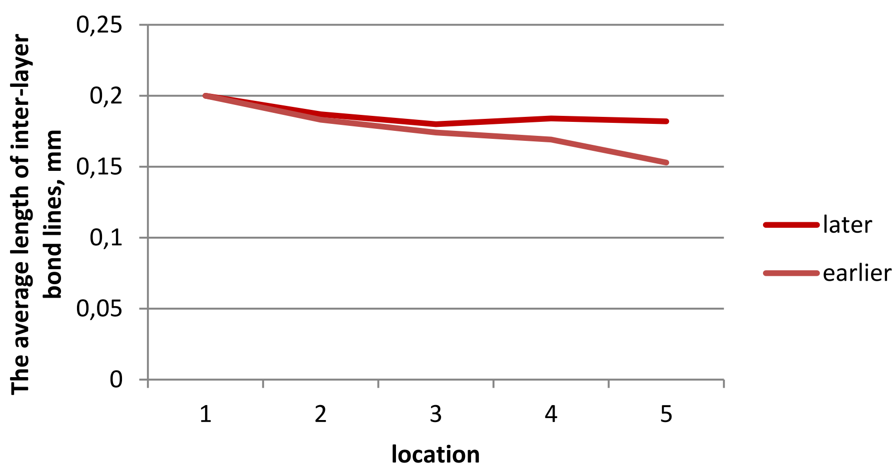

The average length of inter-layer bond lines in different cross-sections

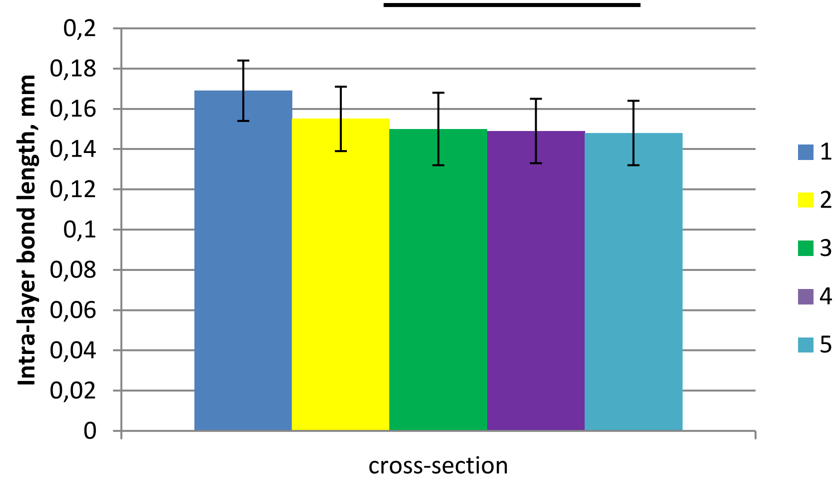

The average length of intra-layer bond lines in different cross-sections

4.Experimental results and discussion

- Results in CT depends on how the boundary is determined.

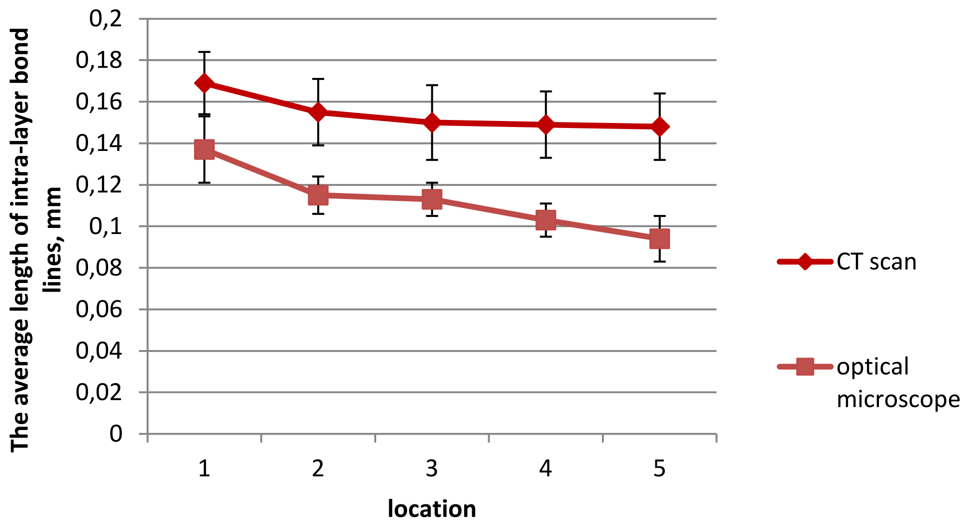

Difference between results from optical microscope and CT scan

Effect of focus spot size on the sharpness of images

4.Experimental results and discussion

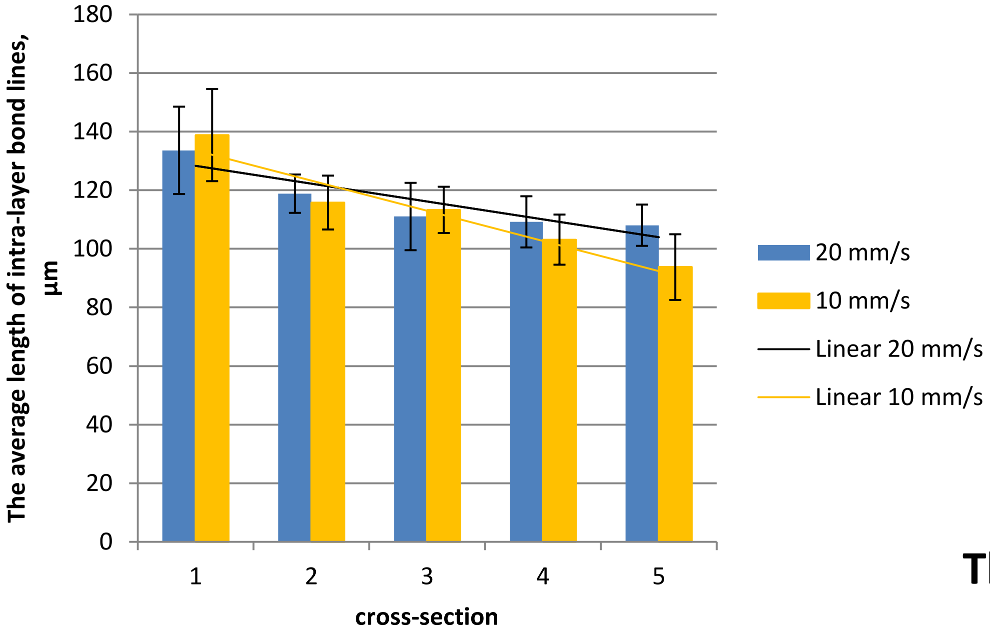

The average length of intra-layer bond lines in 5 cross-sections at different printing speed

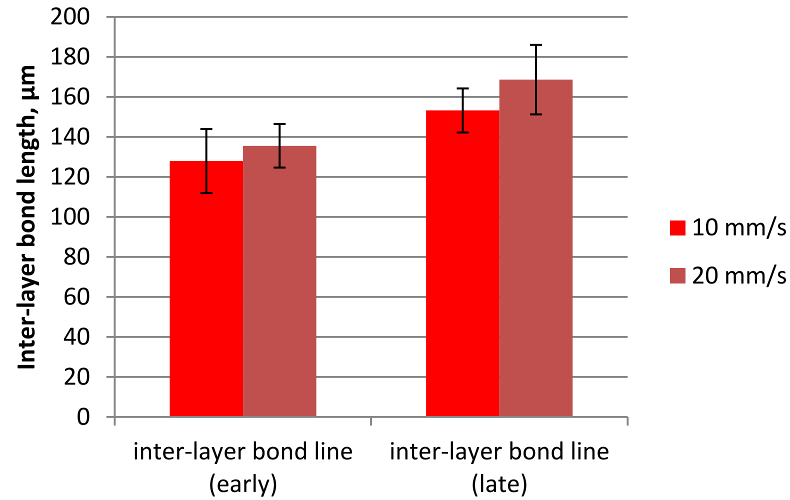

The average length of inter-layer bond lines at different printing speed

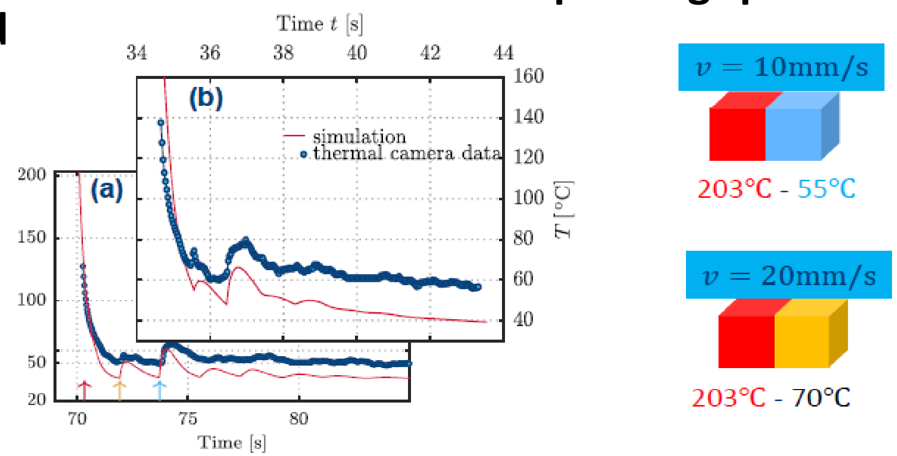

Temperature profile of filament deposition at different printing speed

4.Experimental results and discussion

Mass flow rate = mass/ printing time, [g/s]

Printing time was 121 seconds

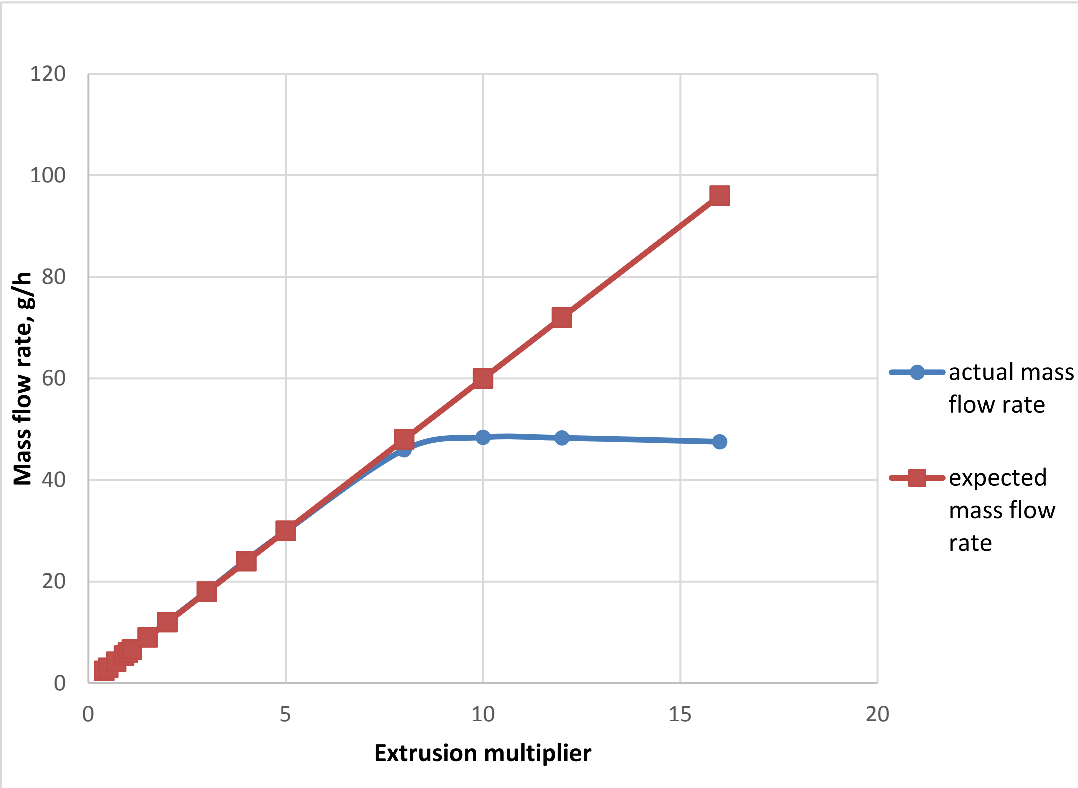

Expected and actual mass flow rate at different EM

- Extrusion Multiplier (EM) allows to control how much filament comes out of the nozzle (feed rate)
- Max print speed 200 mm/s
- You cannot print at this speed with 0.3 mm layer height
- You can print at this speed with max layer height 0.12 mm

$$Limit\ printing\ speed = \frac{mass\ flow\ rate}{3.6 \cdot density \cdot nozzle\ diameter \cdot layer\ height}, [mm/s]$$

$$Limit\ printing\ speed = \frac{45.9}{3.6 \cdot 1.24 \cdot 0.4 \cdot 0.3} = 85.68, [mm/s]$$

4.Experimental results and discussion

- The porosity of the part becomes lower with higher extrusion multiplier, but the thickness of the part grows with increasing EM.

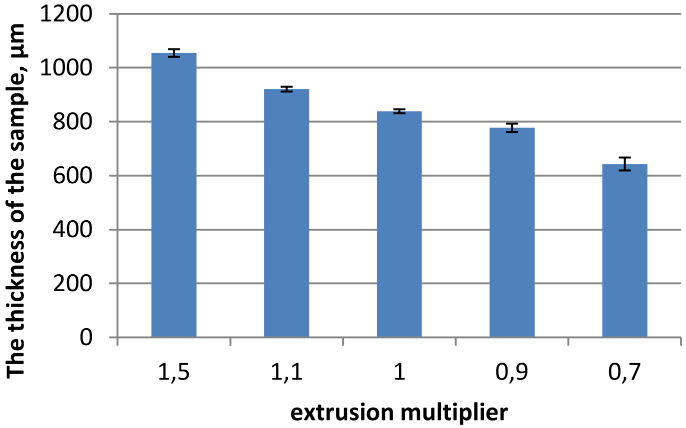

The thickness of the sample at different EM

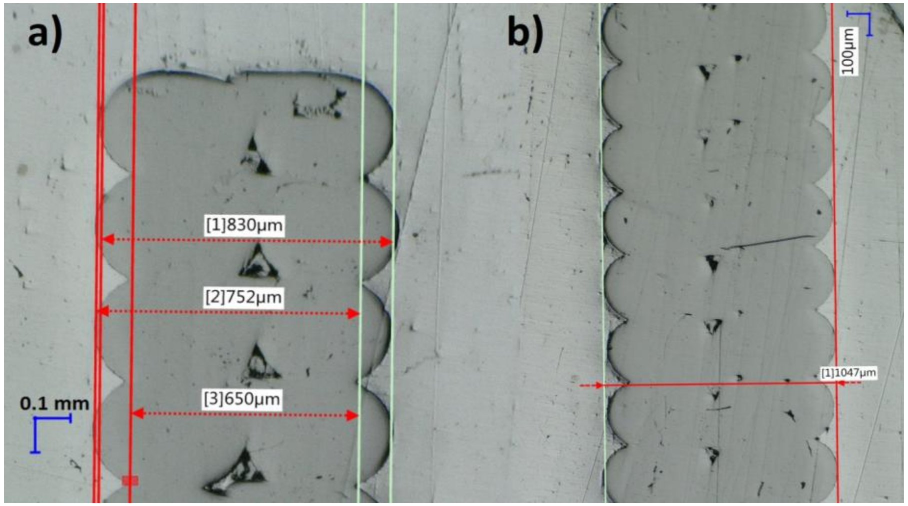

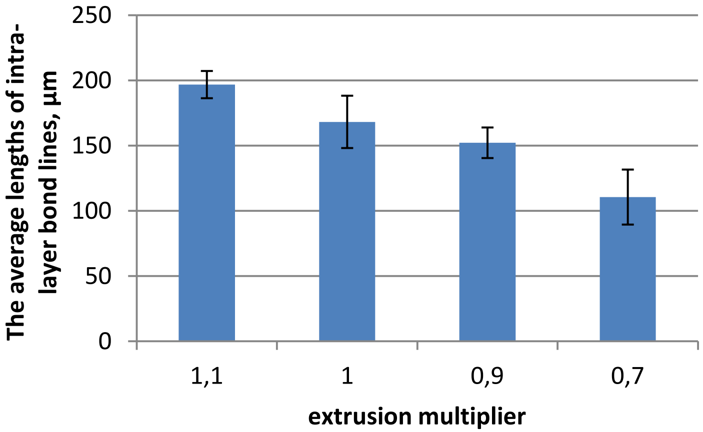

The average length of intra-layer bond lines

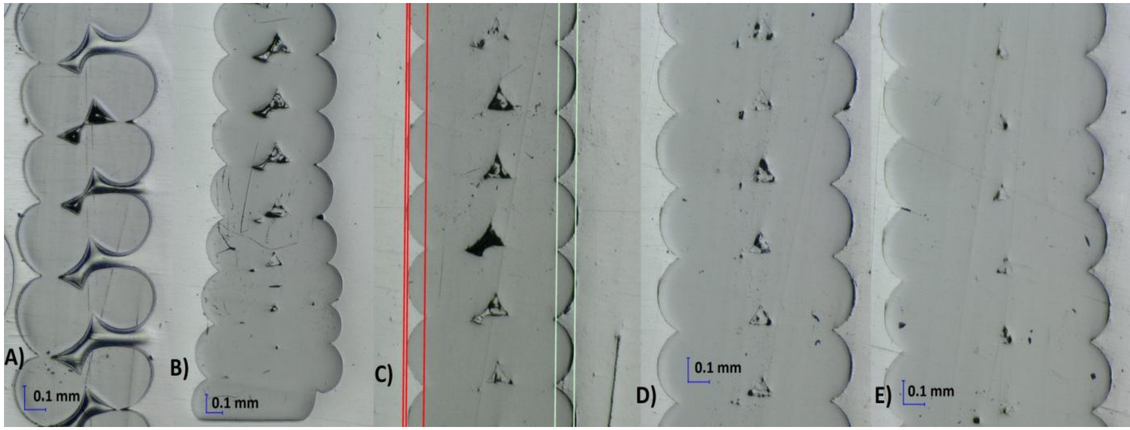

Mesostructure at different EM

4.Experimental results and discussion

- Three values of nozzle-bed distance shift: 0;+0.8;-0.3

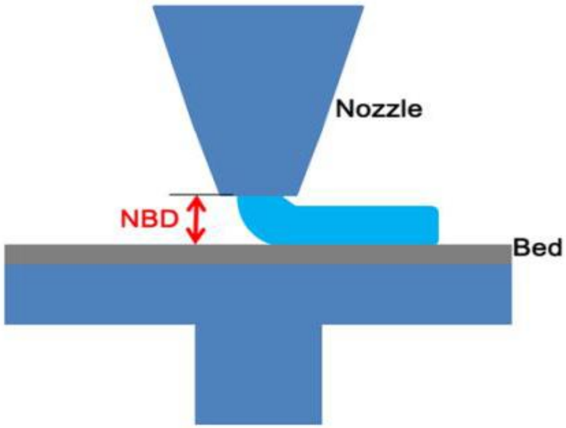

Nozzle-bed distance (NBD)

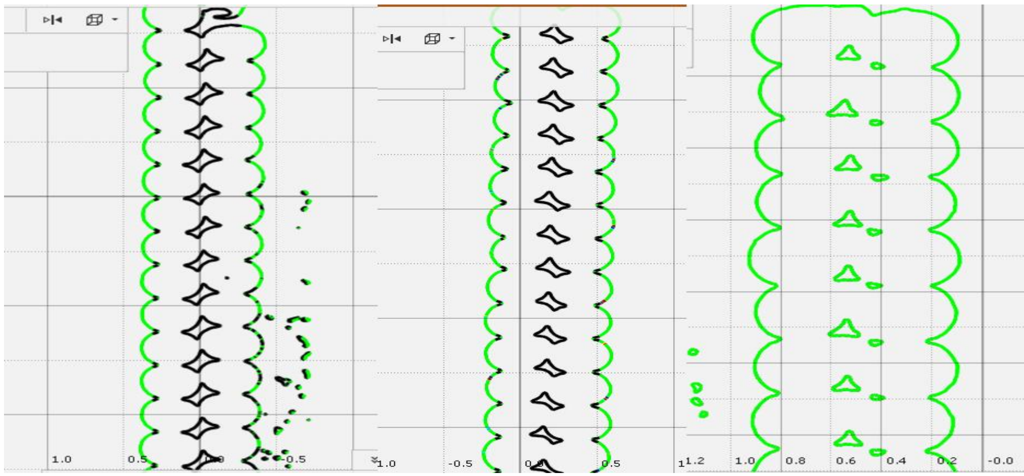

Mesostructure of the samples printed at different NBD (top layers)

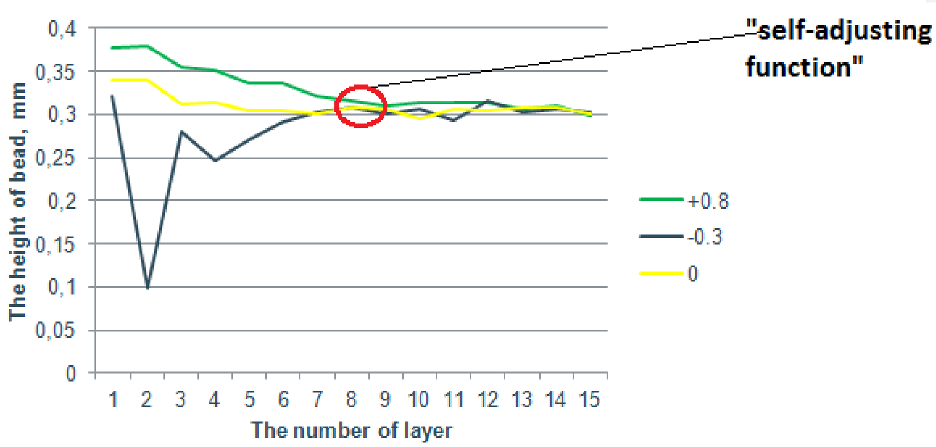

The height of each layer at different NBD

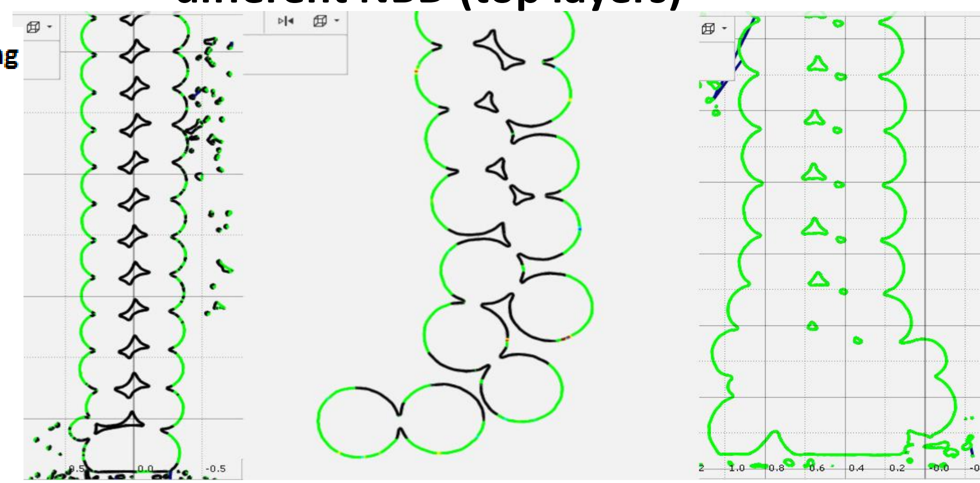

Mesostructure of the samples printed at different NBD (bottom layers)

5.Conclusion

•The shorter intra-layer time - the longer intra-layer bond (shorter inter-layer time - longer inter-layer bond)

•The machine (Prusa i3MK3, nozzle diameter 0.4 mm) can not print faster the mass flow rate 45.9g/h. (85.68 mm/s speed limit for 0.3mm layer height),
(for 200mm/s, layer height need to be lower than 0.12 mm)

•The higher the Extrusion multiplier - benefits: the longer bond lines, the smaller porosity; consequence: deviation from original dimension

•Nozzle-bed distance (NBD) shift has significant effect on the first 6-8 layers (1.8-2.4 mm).

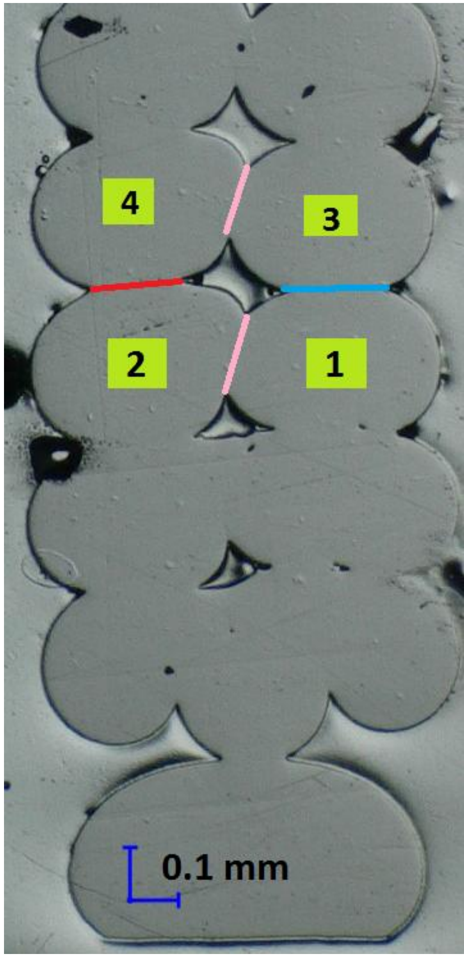

Thank you for your attention!

Any question?